SBDD: kinase inhibitors

Example of SBDD: Imatinib

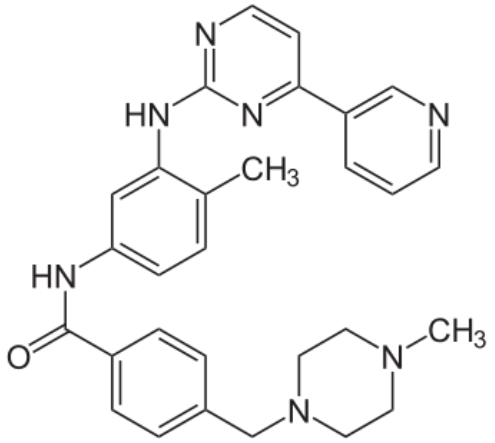

- Imatinib: inhibitor of Bcr-Abl kinase.
- Was developed by SBDD in the late 1990s by biochemist Nicholas Lydon, a former researcher for Novartis, and oncologist Brian Druker of Oregon Health and Science University (OHSU).

Inibitori di chinasi

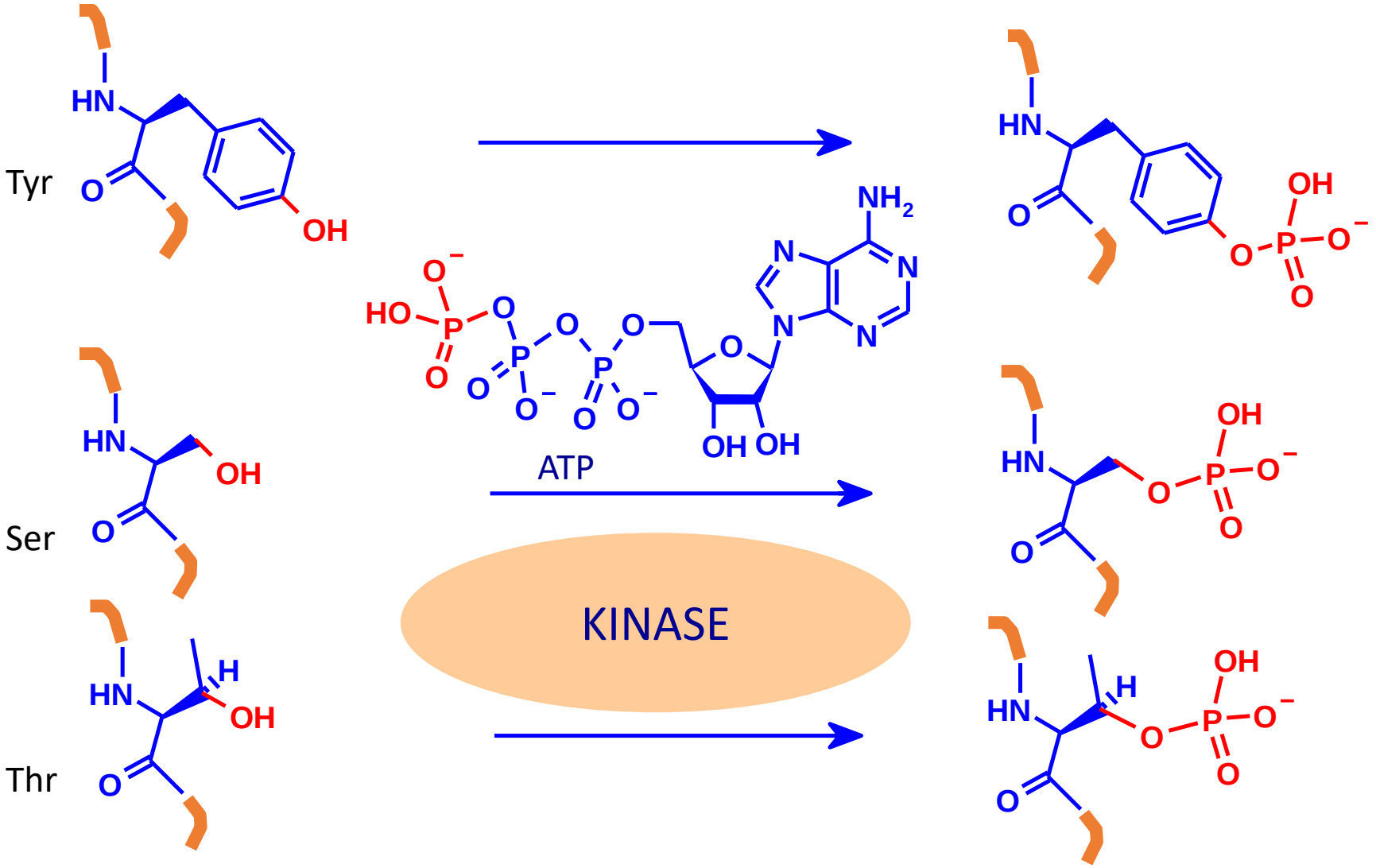

Inhibiting kinases: the selectivity problem

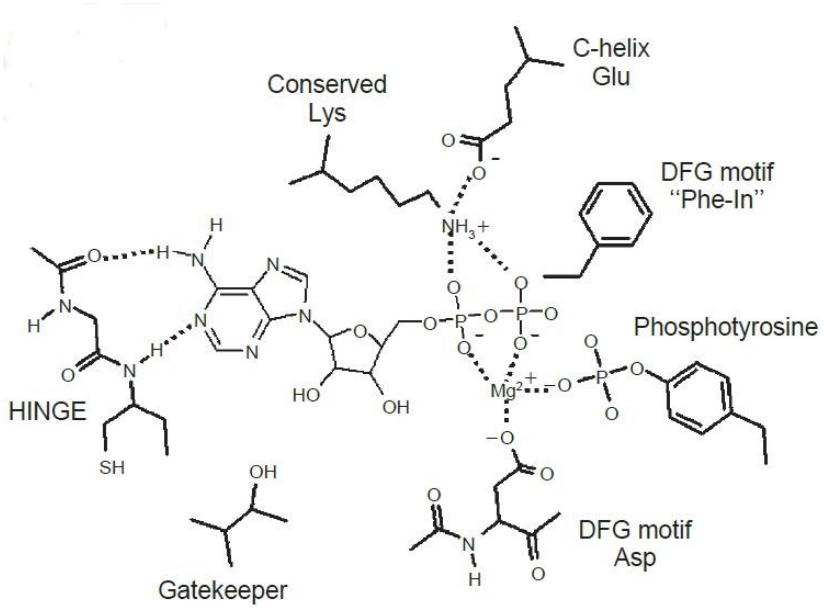

ATP binding site: conserved in all kinases

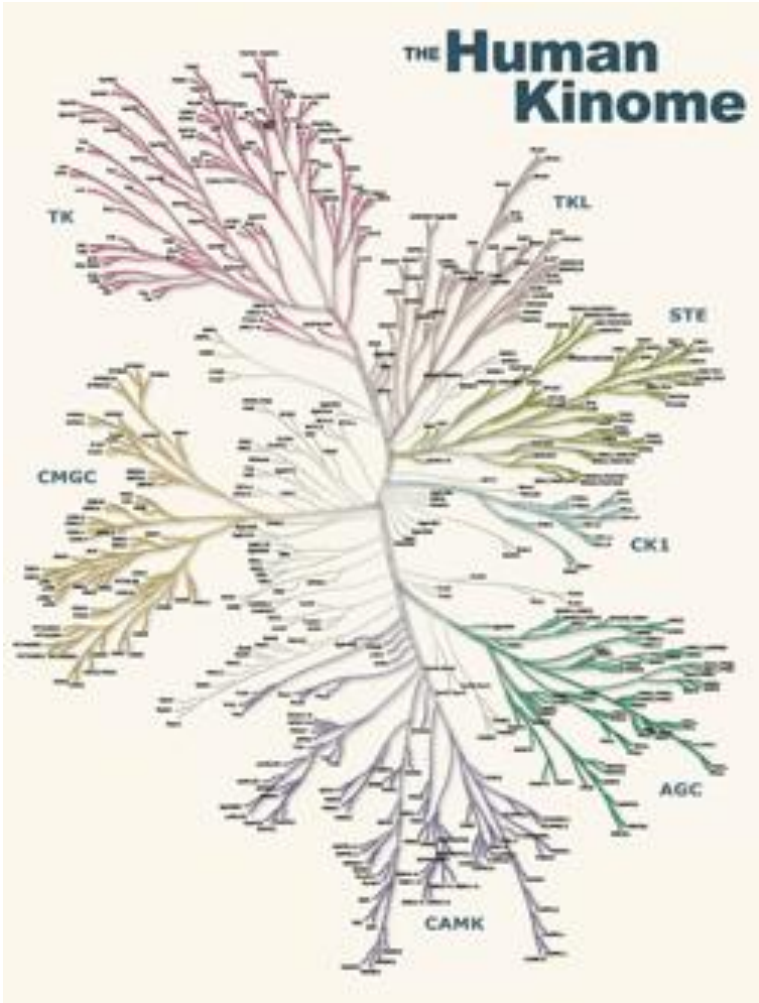

Static representation of the ATP binding pocket, all kinases have a non-conserved hydrophobic pocket

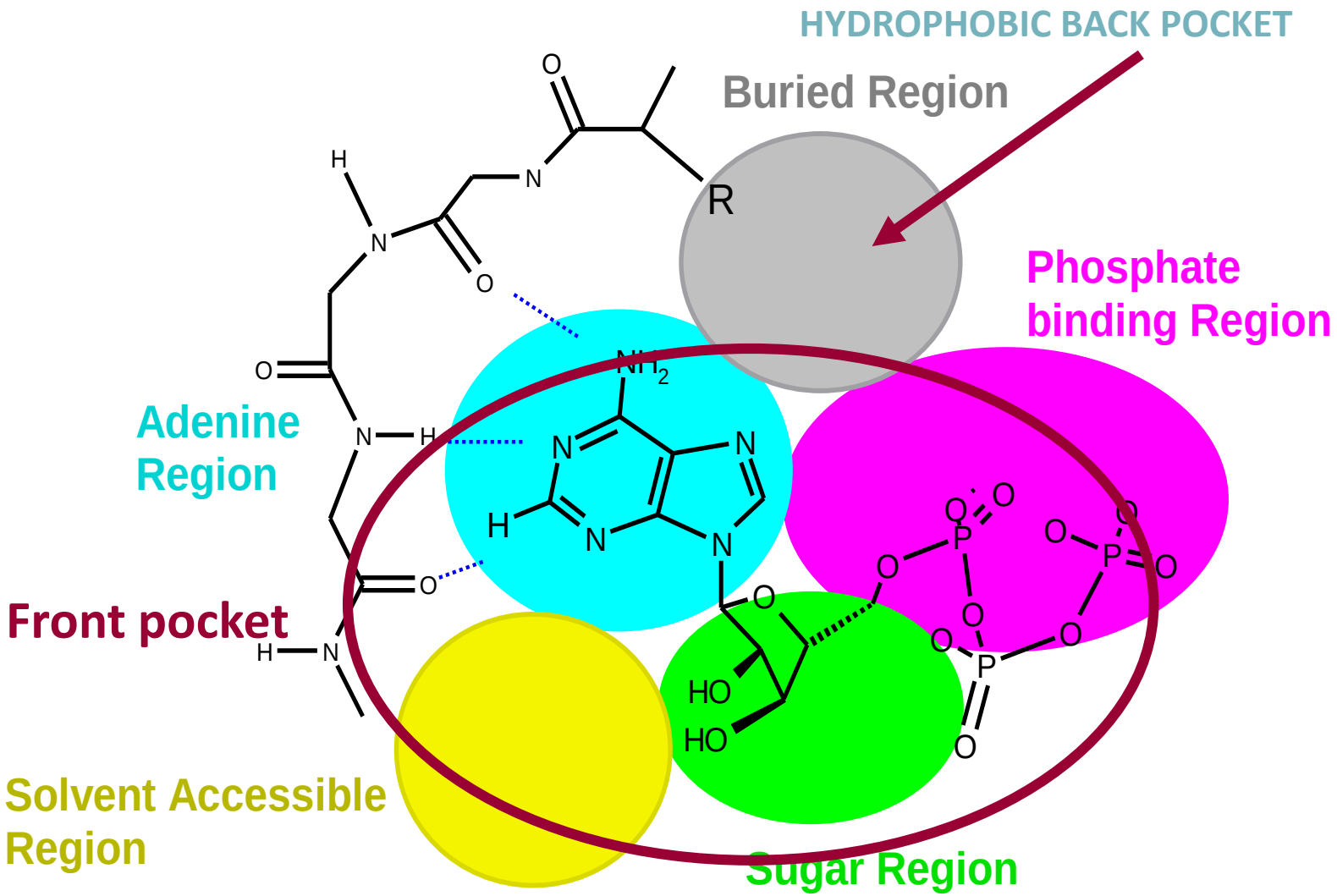

From HIT to LEAD: adding interactions with kinase Bcr-Abl binding pocket (SBDD)

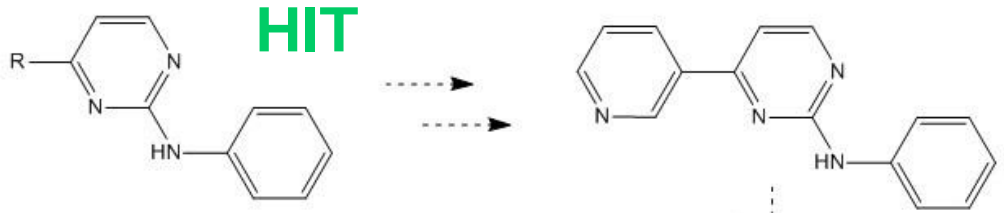

protein Kinases C

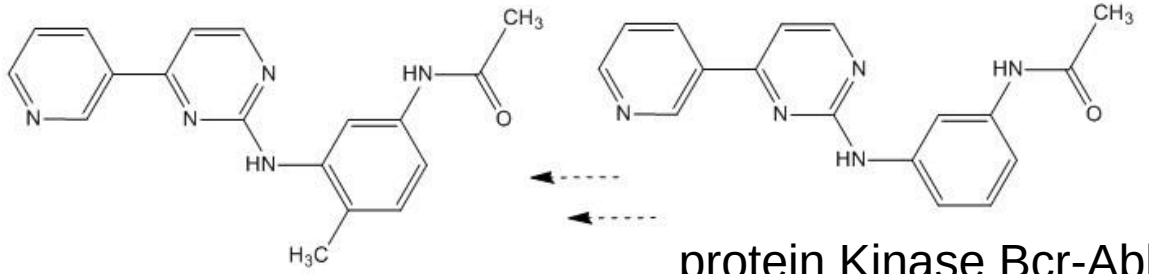

protein Kinase Bcr-Abl

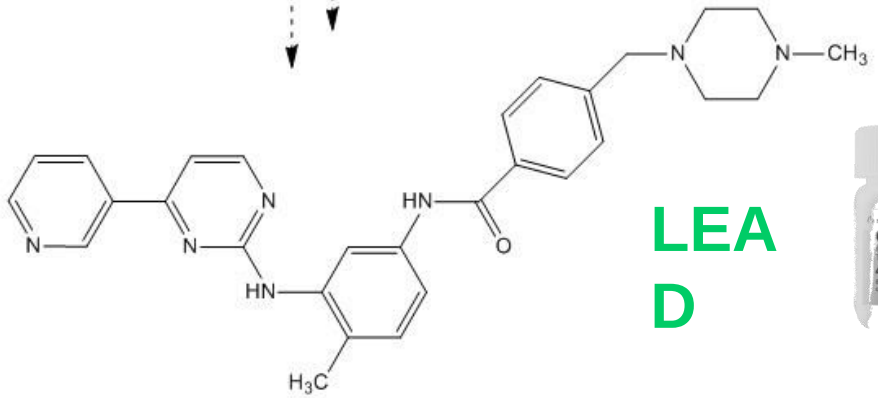

LEAD

Imatininb mesilate
GLEEVEC®

Ligand-protein (drug-target) complexes

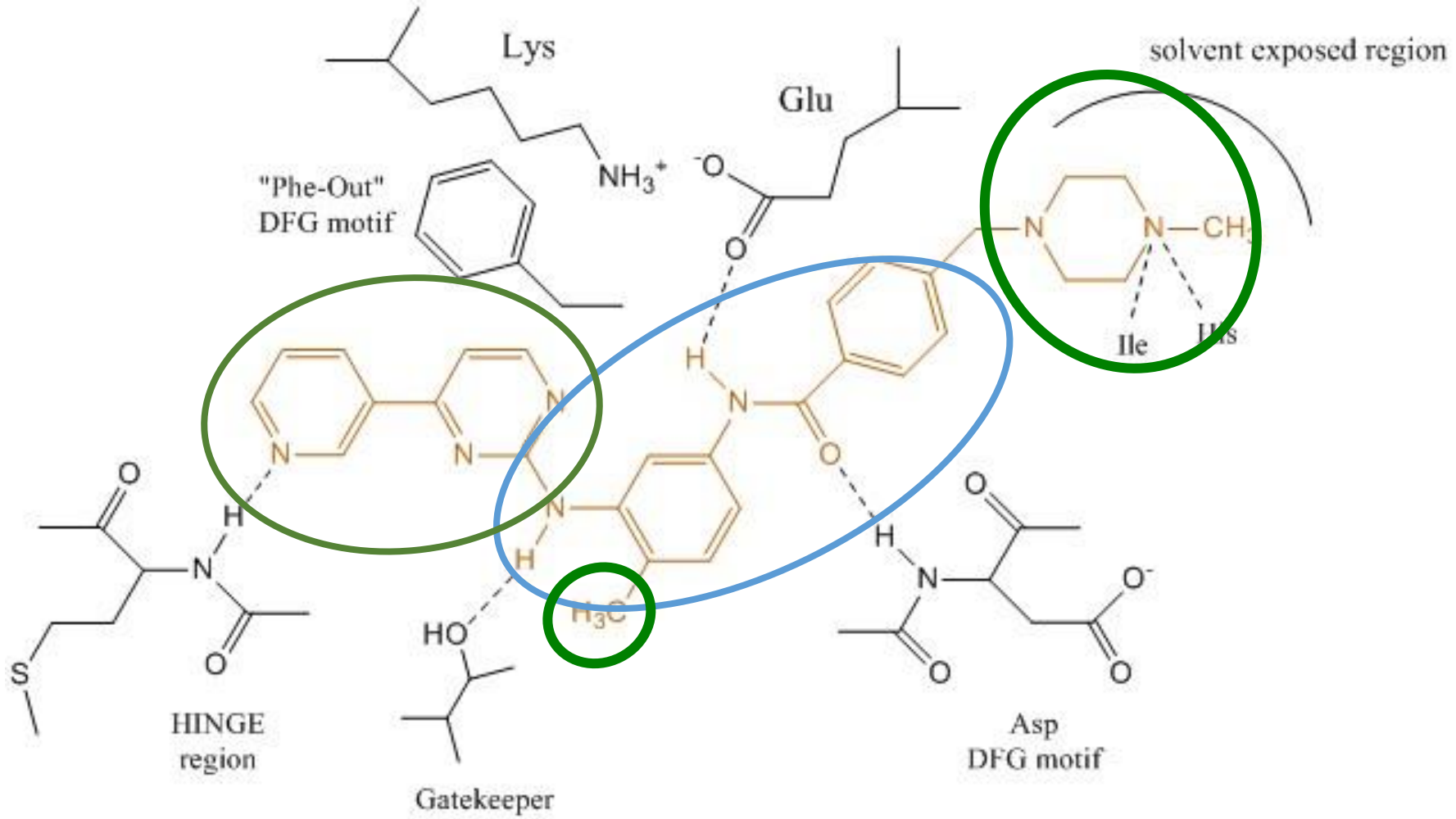

Imatinib in ABL kinase binding site

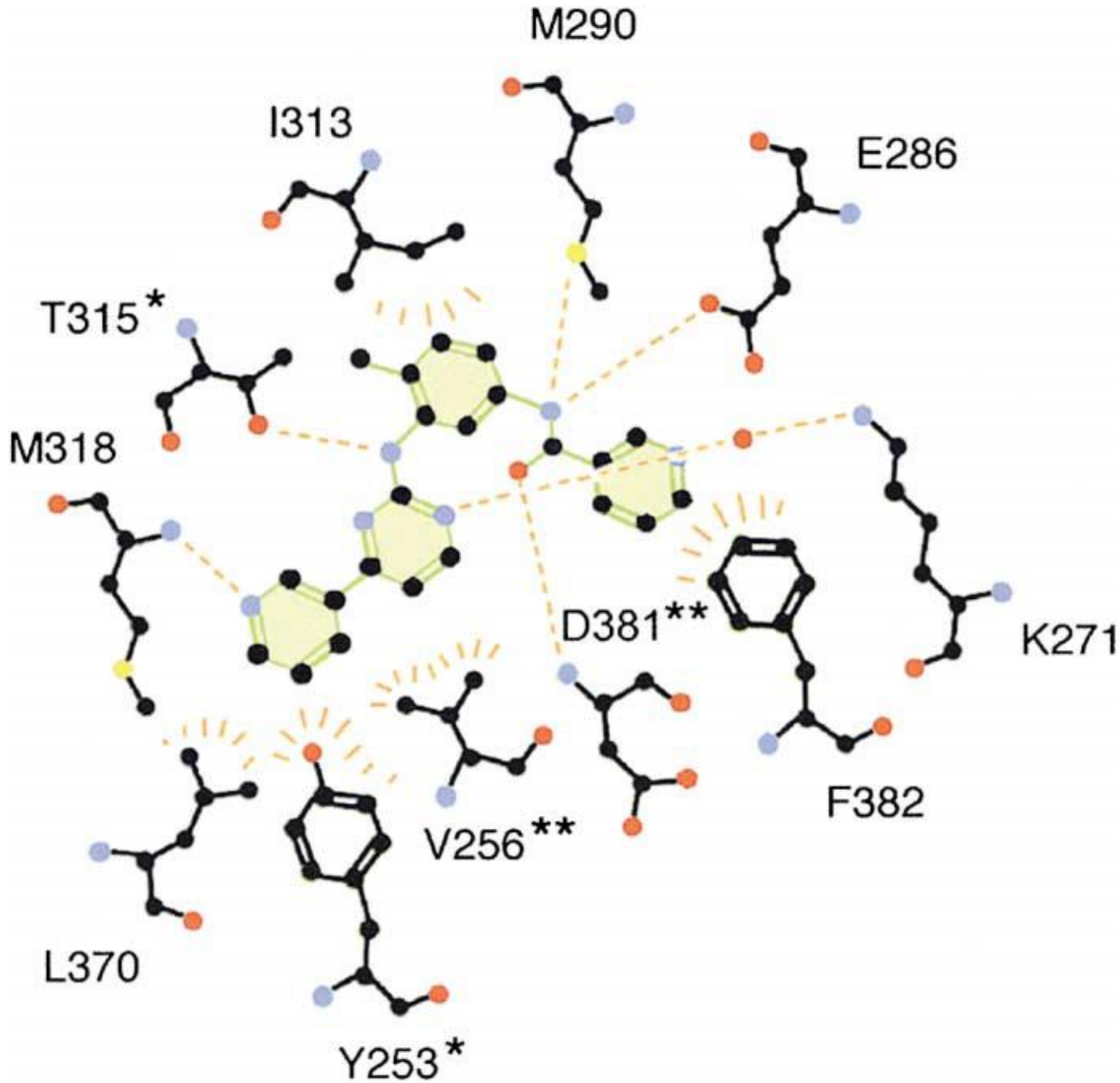
M290
I313
E286
T315*
M318
D381**
K271
F382
V256**
L370
Y253*

- The remarkable success of the targeted cancer drug STI-571, also known as **imatinib**, Gleevec™ or Glivec™, is due to its ability specifically to inhibit disease-causing protein kinases.
- The remarkable clinical success of the Novartis drug STI-571 is seen as a spectacular proof-of-concept for the development of targeted cancer therapies, but in conventional kinase activity screening assays it is a rather unremarkable micromolar inhibitor.

la forma attiva delle chinasi

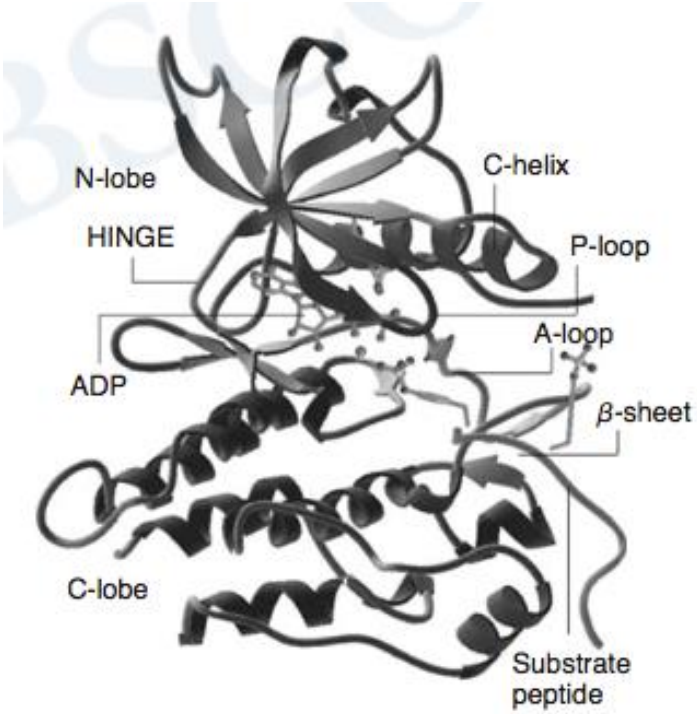

- Consists of the smaller N-lobe (top) and the larger C-lobe (bottom). Key structural elements are shown, including the hinge connecting the two lobes, the C-helix, the phosphate-binding P-loop, the kinase activating A-loop, and the *β*-sheet interaction of the A-loop with the C-lobe that stabilizes the extended A-loop conformation. Also shown as ball-and-stick models are the positions of the bound ADP in the kinase active site, as well as the phosphotyrosine residues of the substrate peptide.

- The active c-Kit structure demonstrates how a number of interconnected structural elements must function together to perform the phosphoryl transfer reaction.

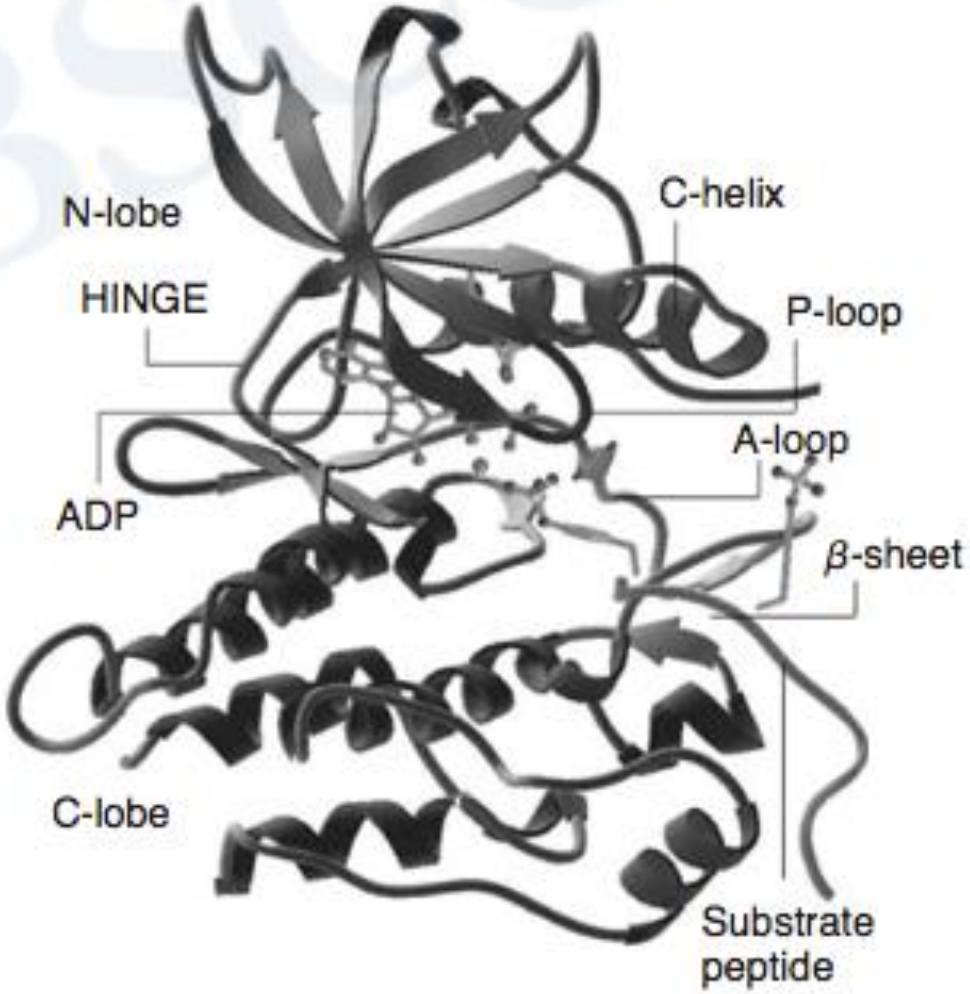

- The C-helix needs to be properly positioned to form the conserved Glu- Lys pair that orients the ATP phosphate groups

la forma inattiva delle chinasi (Autoinhibited c-Kit kinase structure)

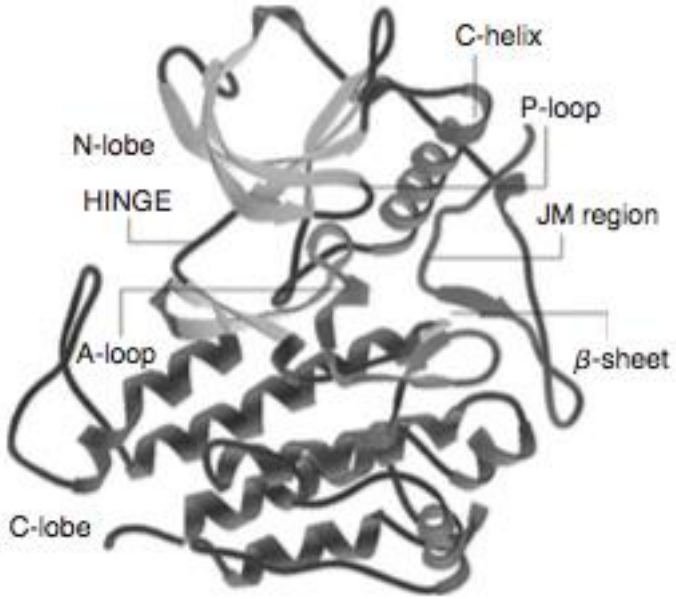

- Autoinhibited c-Kit kinase structure.
- The entire juxtamembrane region is visible in this struc- ture and inserts between the kinase N- and C-lobes, shifting the C-helix, and blocking the A-loop from attaining its active conformation by forming a similar β-sheet with the C-lobe. The autoinhibited A-loop is folded back over the kinase C-lobe rather than in an extended conformation.

- La forma AUTOINIBITA DELLE CHINASI
- the P-loop must also pack with the phosphates and seal the reaction site from solvent.

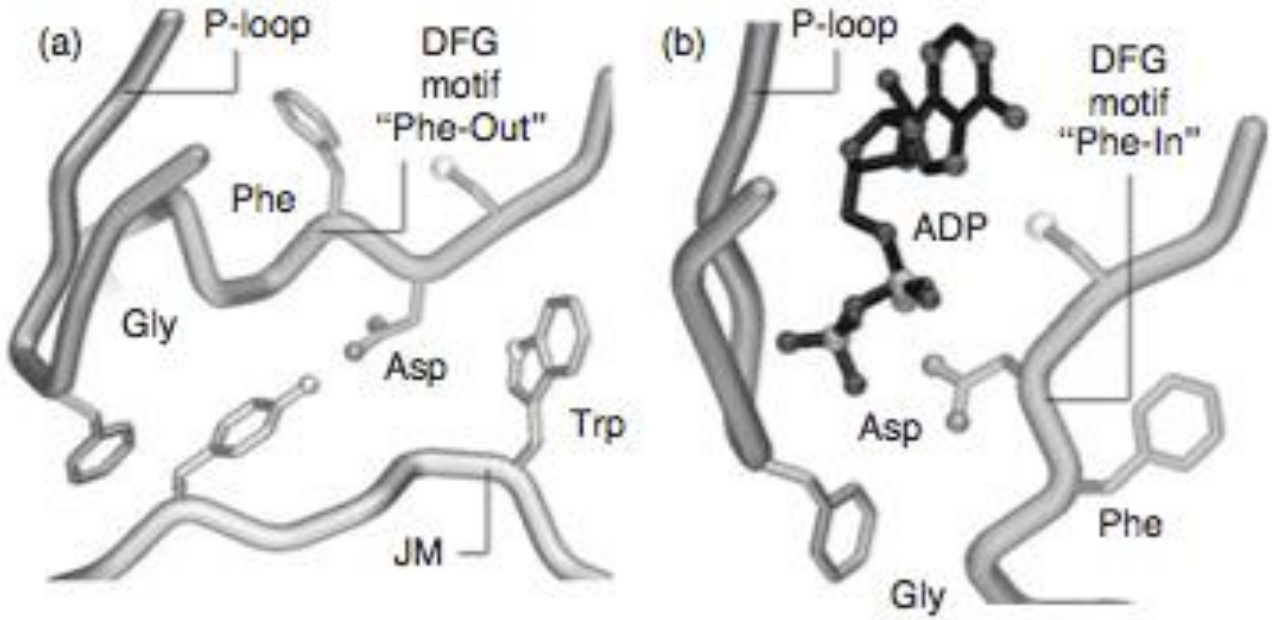

FIGURE 10.6 The c-Kit DFG motif structural switch. (a) Autoinhibited c-Kit kinase. The DFG motif is in the "Phe-Out" conformation, with the inserted TRP residue of the JM region blocking the Phe from its active position. (b) Active c-Kit Kinase. The DFG motif is in the "Phe-In" orientation within the activation loop in an extended conformation.

- The ATP molecule must also be able to access the hydrophobic pocket and interact with the hinge region, and this binding is dictated by the conformation of the DFG motif.
- In the active “Phe-In” conformation, the DFG motif induces the A-loop to assume an extended conformation that is compatible with substrate binding.

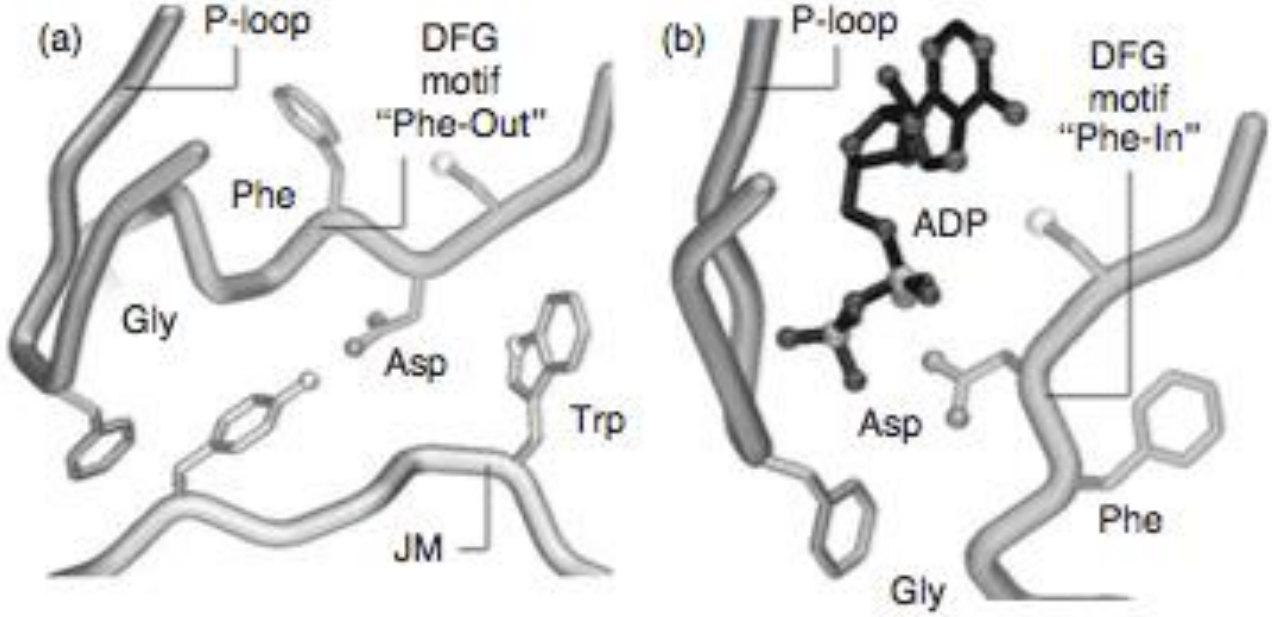

FIGURE 10.6 The c-Kit DFG motif structural switch. (a) Autoinhibited c-Kit kinase. The DFG motif is in the “Phe-

Il binding con ATP e substrato

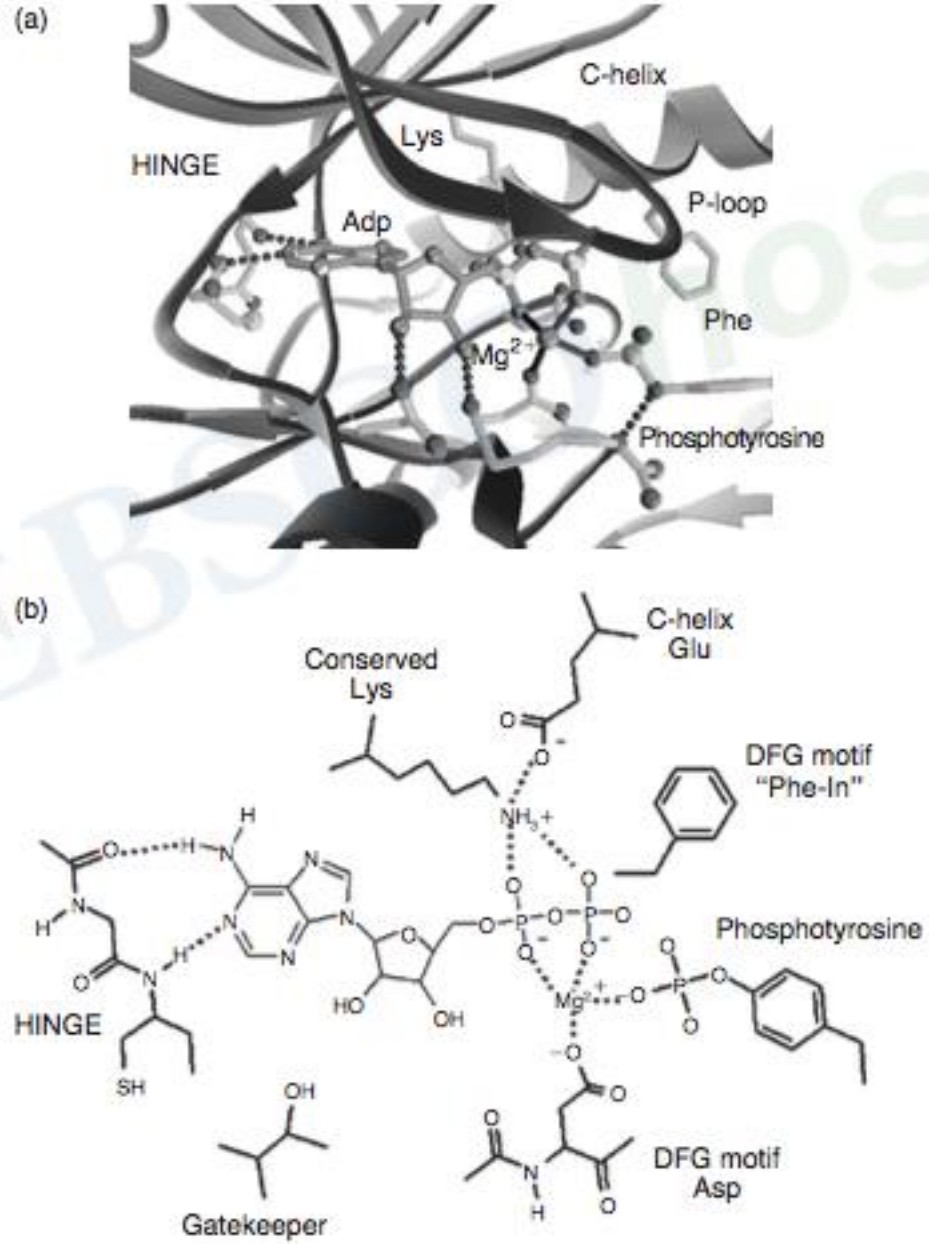

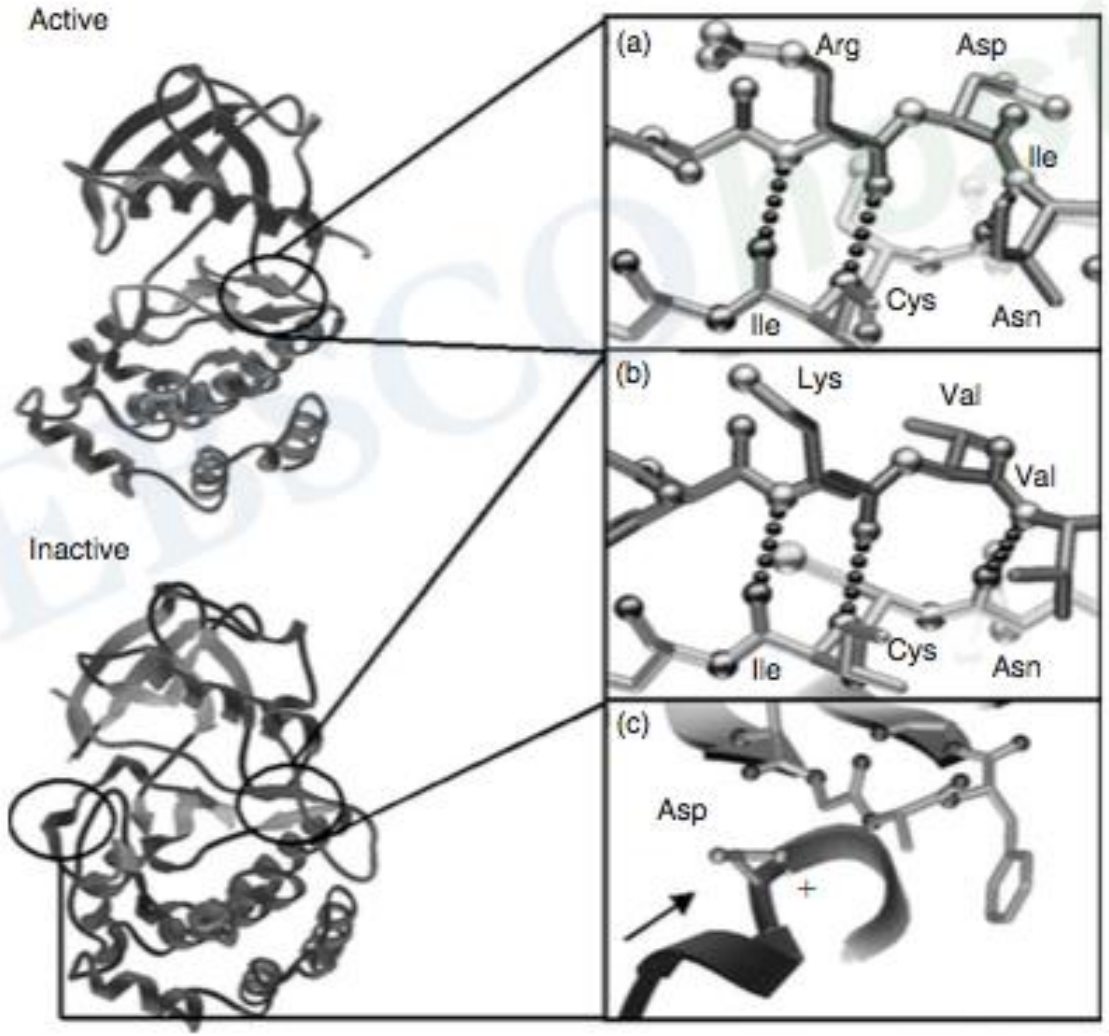

- Stabilizing secondary structure elements in active and inactive c-Kit kinase. Cα ribbon drawings of active (top) and autoinhibited inactive (bottom) c-Kit kinase viewed from the side looking into the interdomain cleft.

Imatinib stabilizes the inactive form of Abl kinase

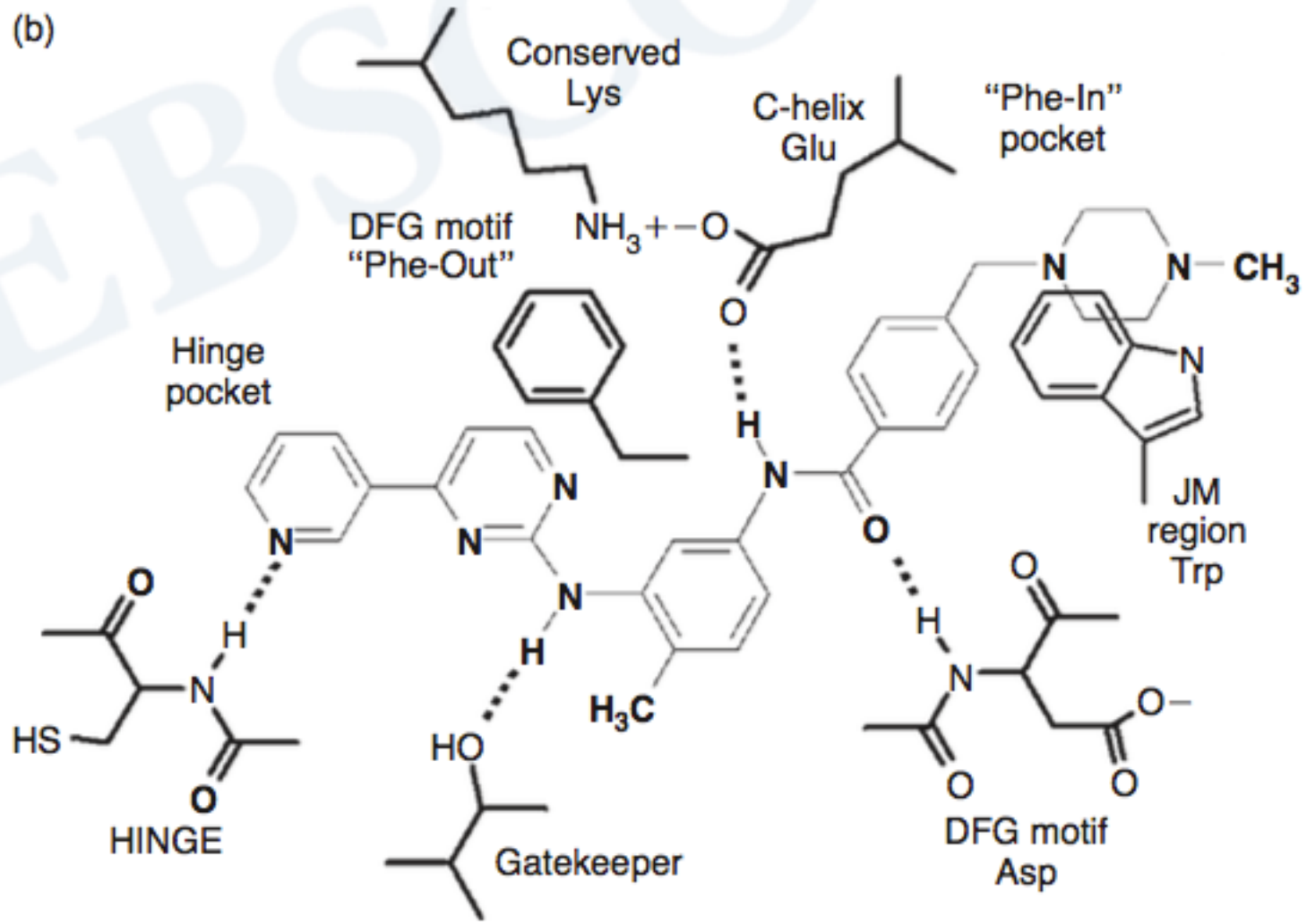

Triazole analogues

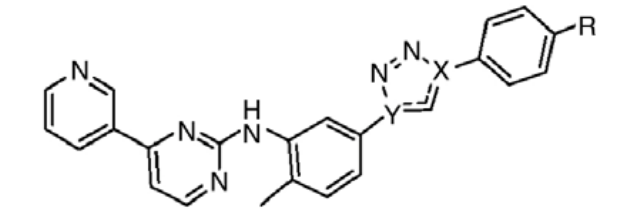

Imatinib triazole analogs
(5)

The activity of 1,2,3-triazole analogs[a,b,c]

Compound	Parent compound	Biological target	Isostere activity evaluation	Parent compound activity evaluation
Amide isosteres				
1	Linezolid	*Staphylococcus aureus*	0.5–1 μg/ml[ii]	0.5–2 μg/ml[ii]
2	Merck compound	BACE1	2.0 μM[iv]	16.3 μM [iv]
3	RN-18	H9 cells (HIV-1 Vif)	0.001 μM[iv]	6 μM [iv]
4	Amprenavir	HIV-1Pr $_{wt}$	6 ± 0.5 nM[iv]	–
		HIV-1Pr $_{6X}$	15.7 nM[iv]	–
5	Imatinib	K562 (Bcr-Abl)	0.89 ± 0.003 μM[iv] 0.03 μM[iv]	0.37 ± 0.09 μM[iv] 0.38 μM[iv]

inibitori di chinasi

- Tipo I: agiscono sulla forma attiva (Phe-in) e competono con il substrato o il cofattore (ATP) per il binding con il sito attivo
- Esempi: gefitininb, erlotinib
- Tipo II: si legano alla conformazione inattiva (Phe-out) e la stabilizzano.
- Esempi: Imatininb, lapatinib, sorafenib.

Inibitori tipo I

Gefitinib

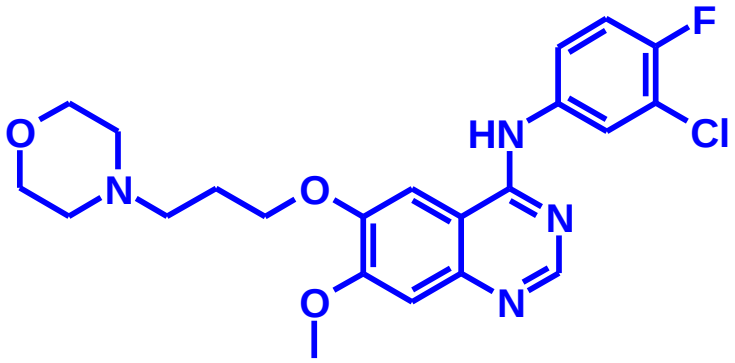

Iressa (EGFR inib.)

(Astra-Zeneca)

Registrato per tumore NSCL

(Non-small cell lung cancer)

Erlotinib

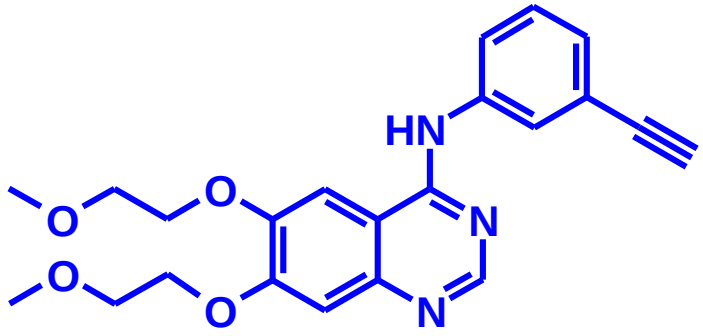

Tarceva (EGFR inib.)

(OSI Pharmaceuticals)

in Fase III

Per diversi tipi di tumori fra cui tumore NSCL e tumore pancreatico

Inibitori tipo II

Lapatinib

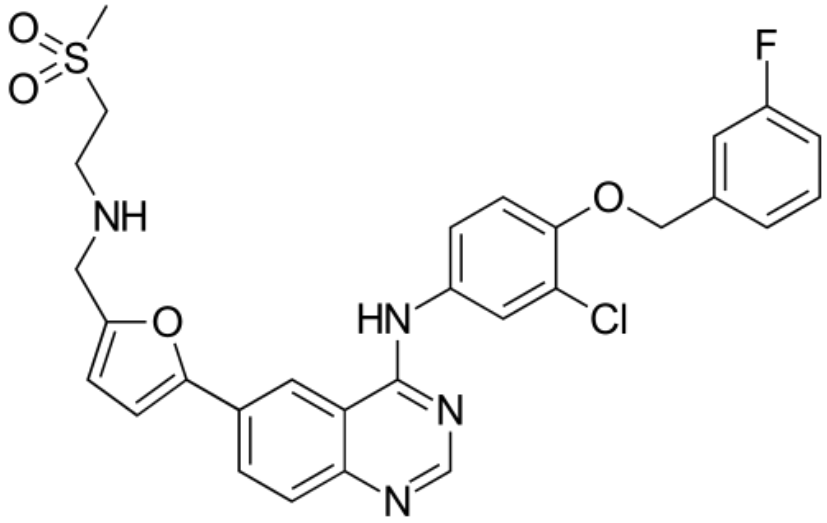

Sorafenib

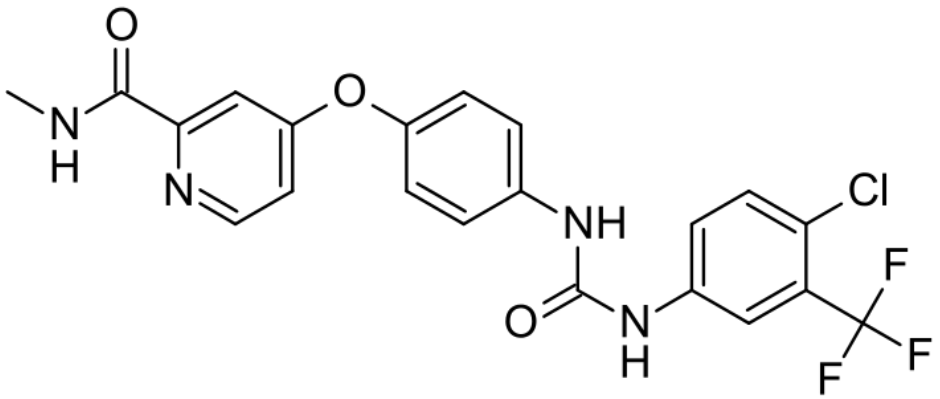

Abrocitinib (Cibinqo ®)

A selective JAK1 inhibitor developed by Pfizer for the treatment of moderate-to-severe Atopic Dermatitis

CIBINQO™
(abrocitinib) tablets 50mg 100mg 200mg

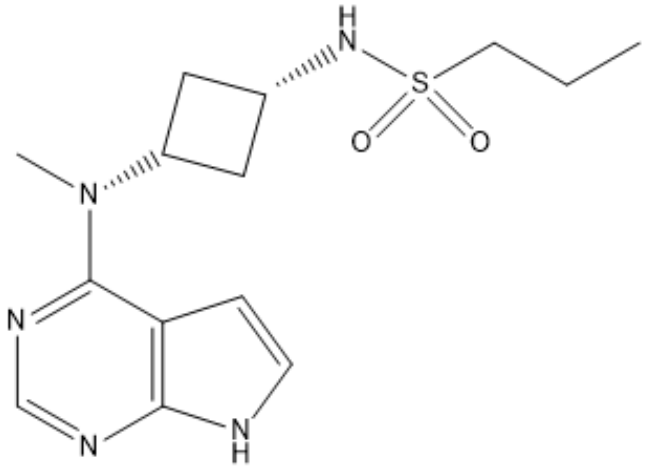

Atopic Dermatitis

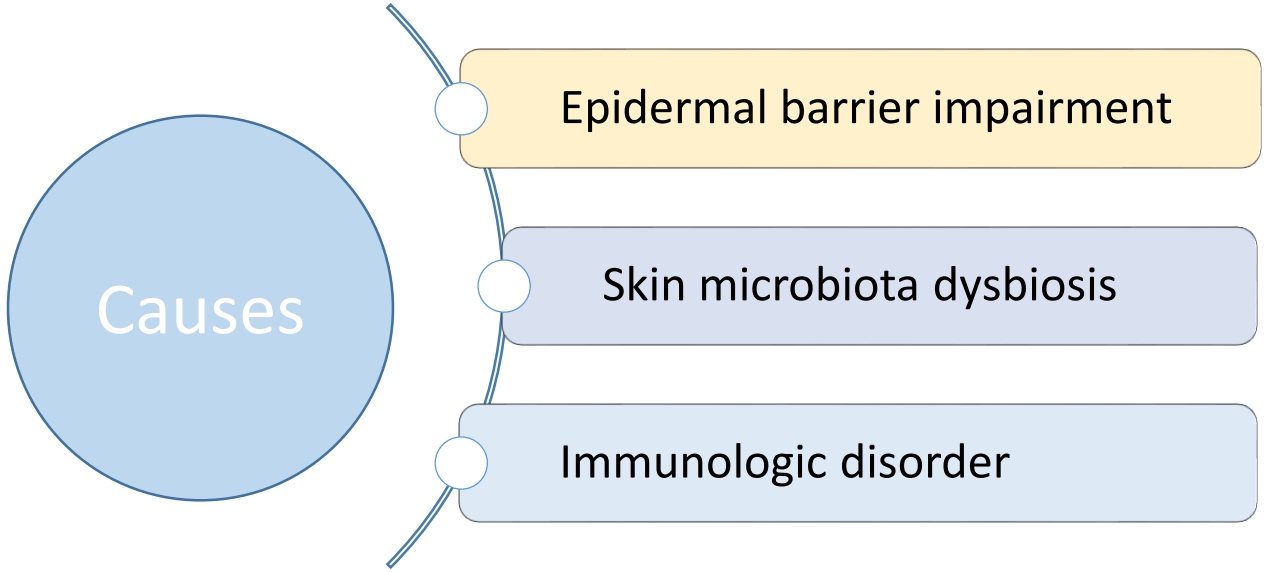

Atopic Dermatitis

Causes

- Epidermal barrier impairment
- Skin microbiota dysbiosis
- Immunologic disorder

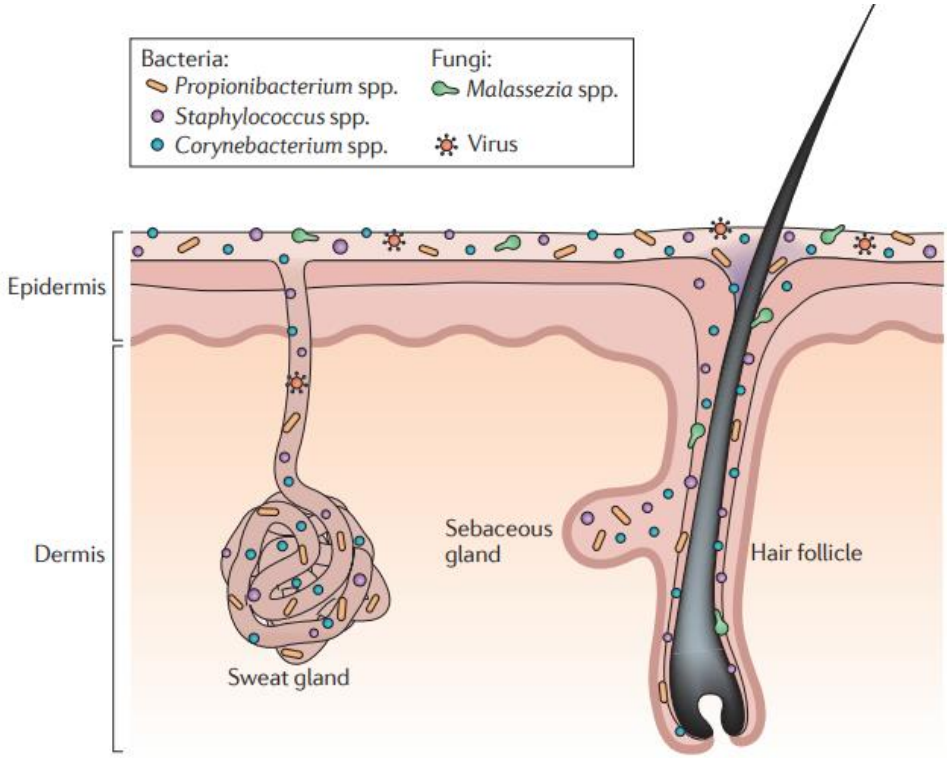

Atopic Dermatitis

Causes

- Epidermal barrier impairment
- Skin microbiota dysbiosis
- Immunologic disorder

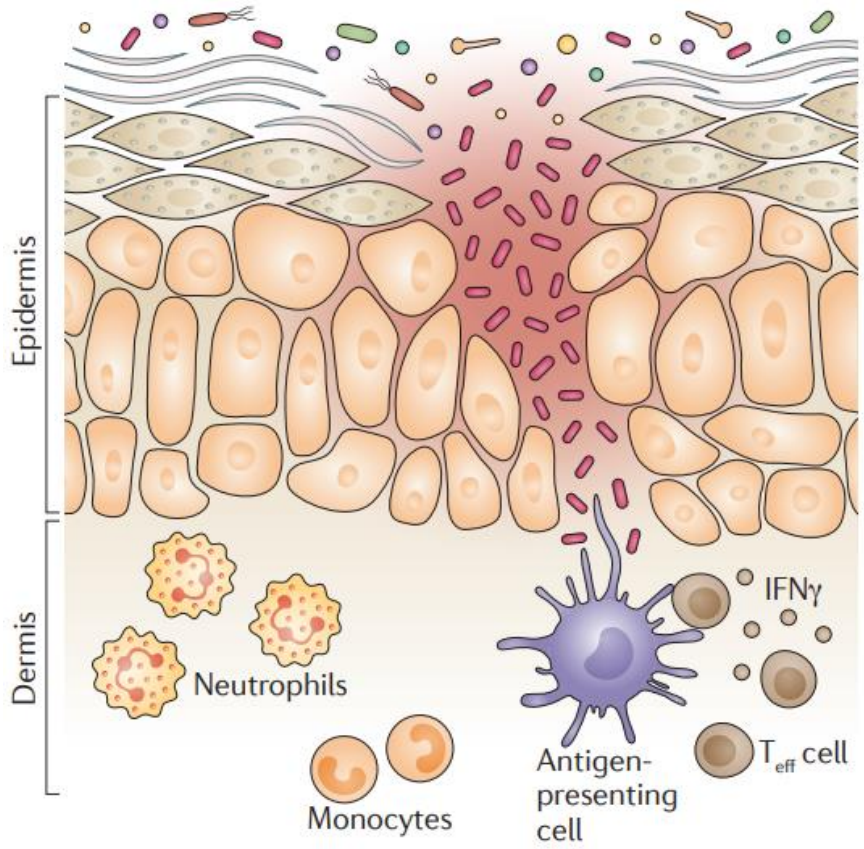

JAK/STAT pathway

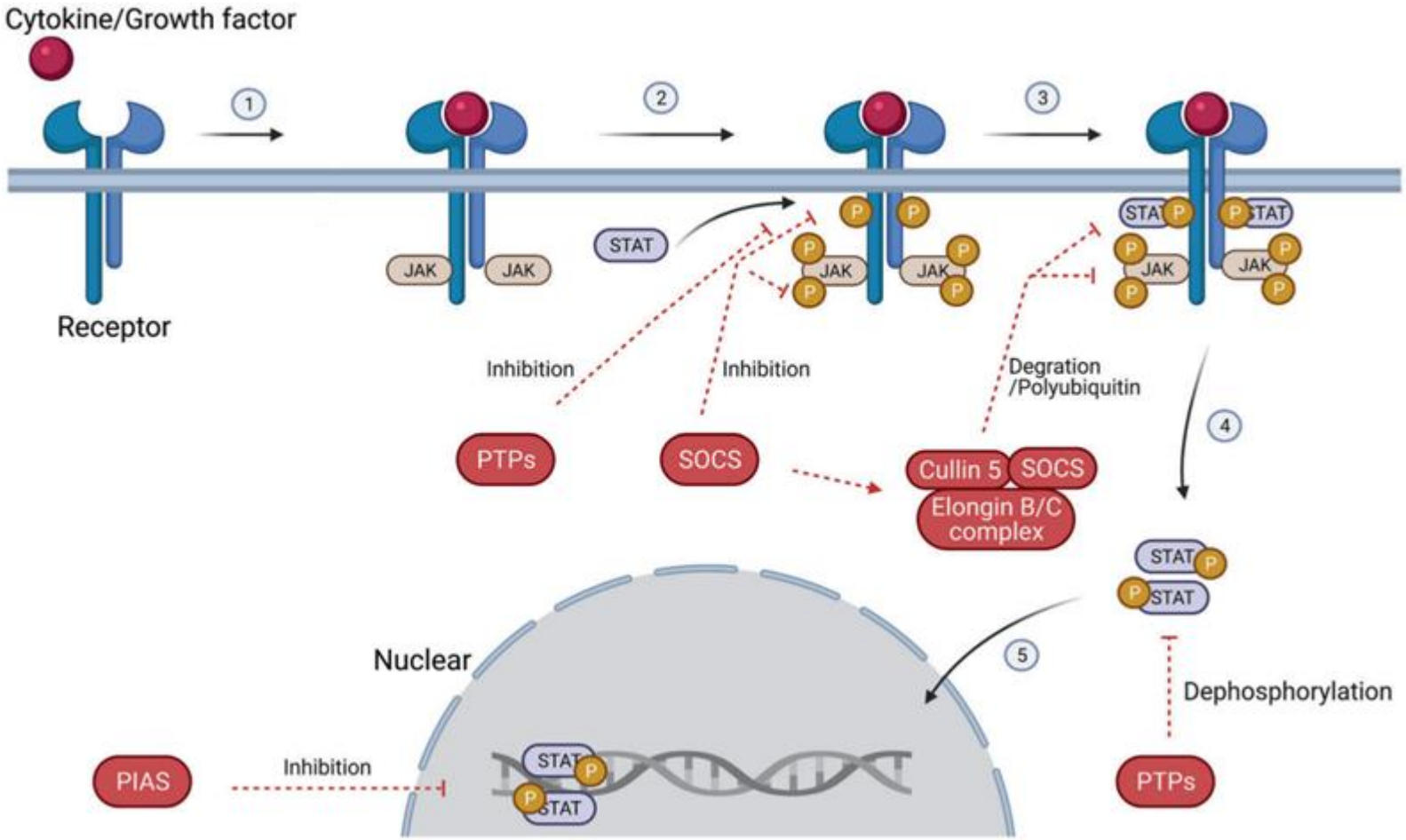

JAK: Janus Kinase

STAT: Signal Transducer and Activator of Transcription

Target: JAK family

JAK1: major role in the signaling of proinflammatory cytokines

JAK2: interaction with receptors for hematopoietic growth factors

JAK3: primary role in mediating immune function

TYK2: regulation of antiviral and inflammation response

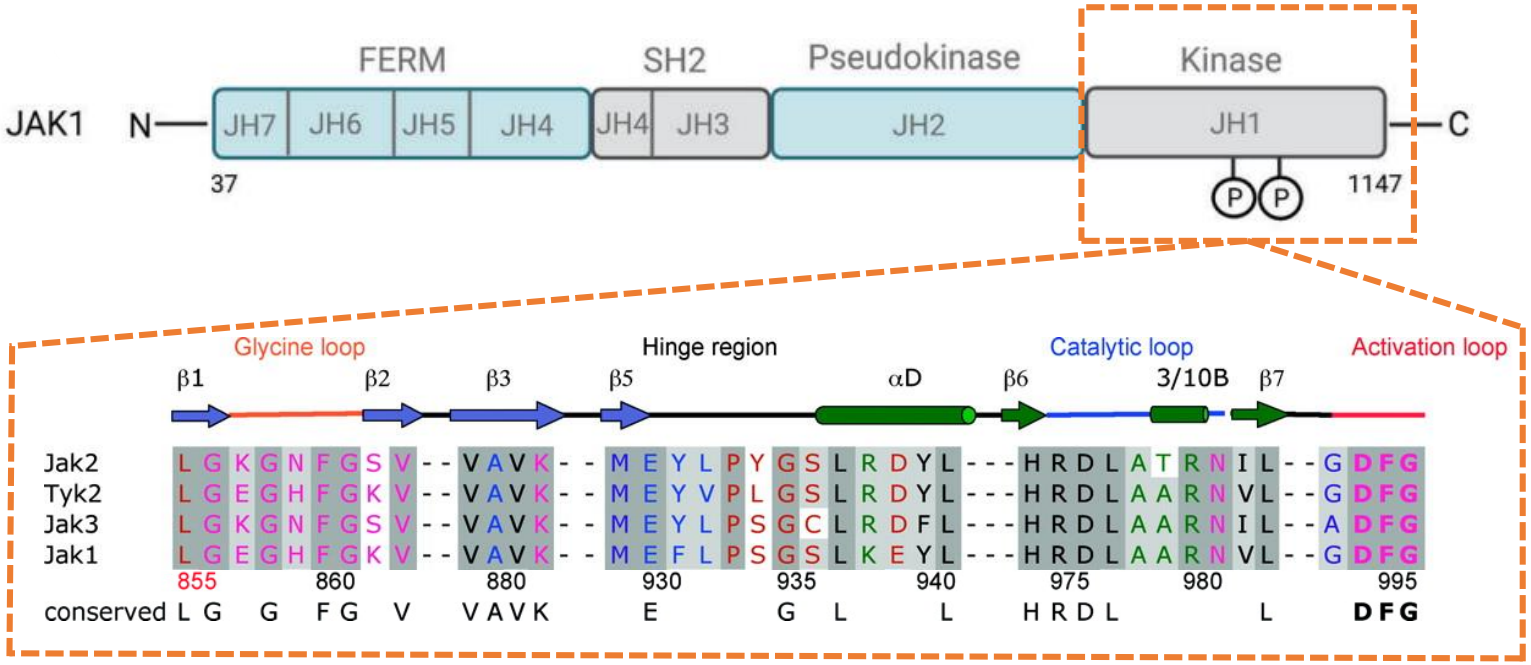

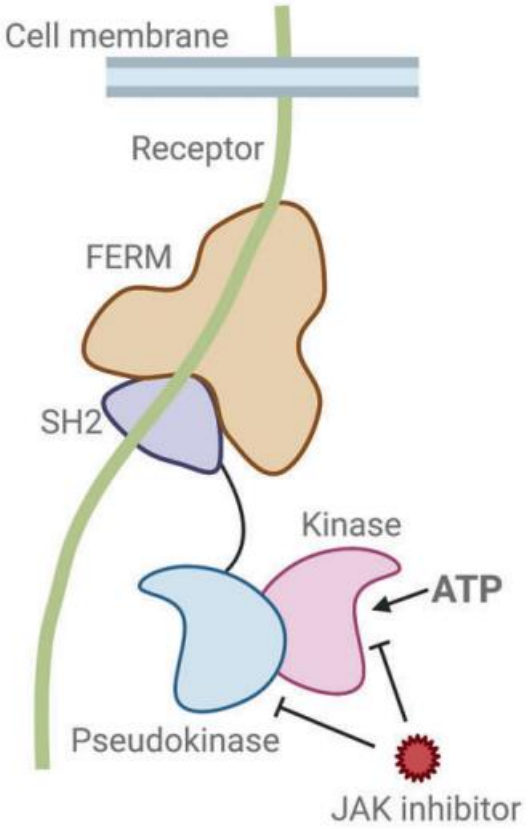

JAK1-ADP

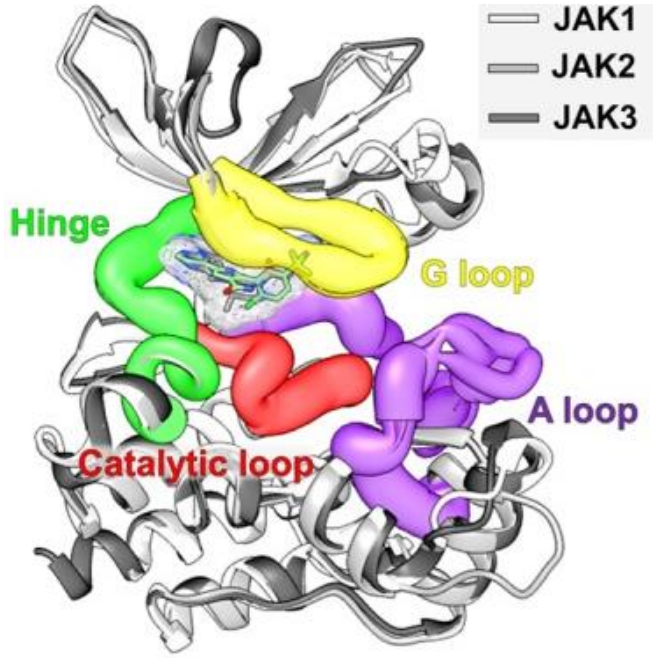
JAK1
JAK2
JAK3
Hinge
G loop
A loop
Catalytic loop

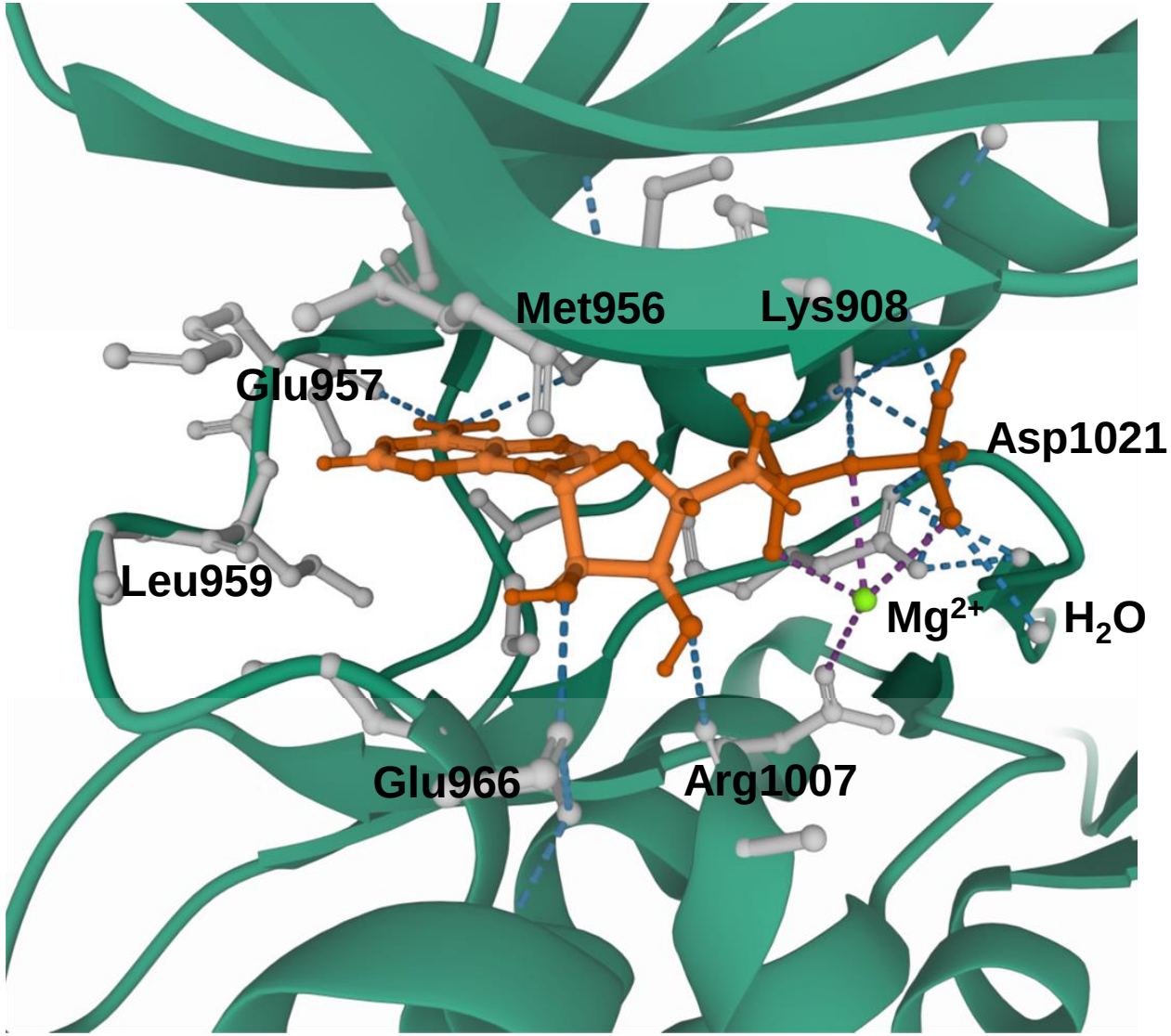
Met956
Lys908
Glu957
Asp1021
Leu959
Mg^{2+}
H_2O
Glu966
Arg1007

JAK1-ADP

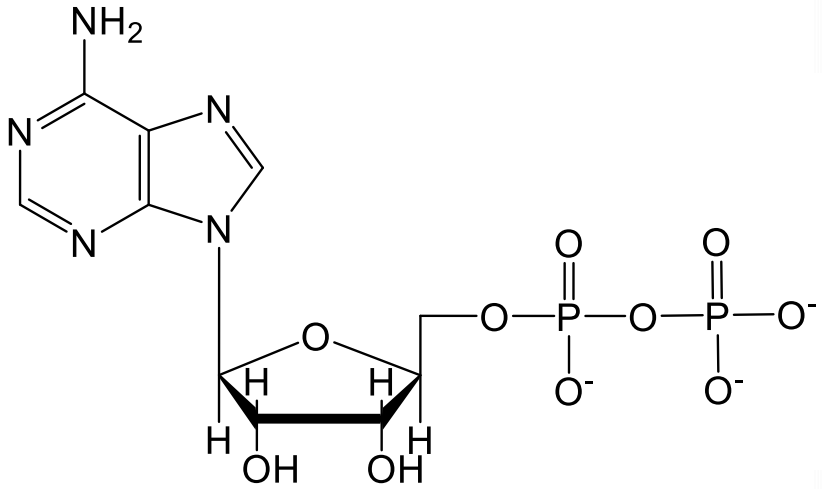
NH2
N
N
N
N
O
H
H
H
H
OH
OH
O
P
O
P
O
O
O-
O-
O-

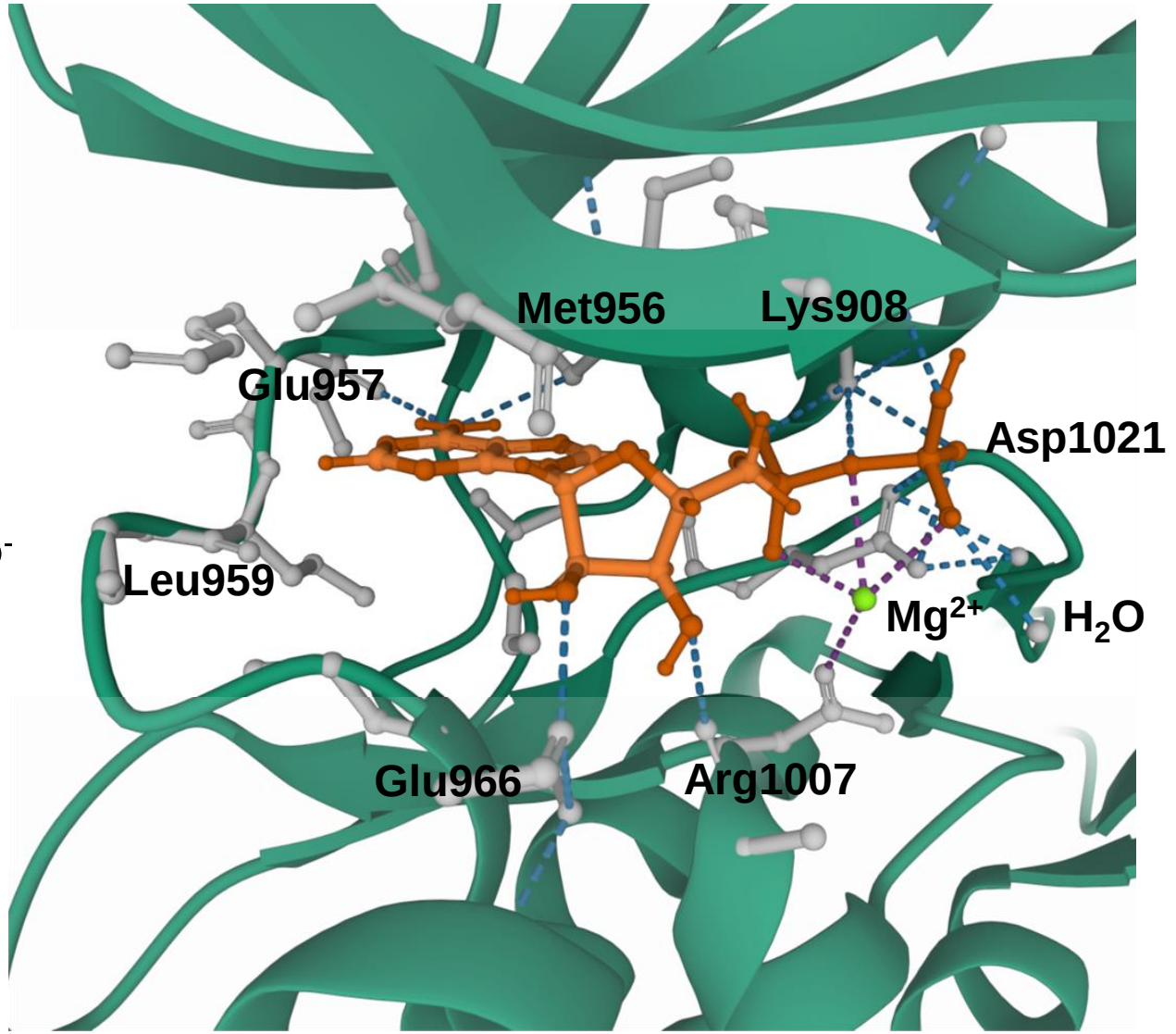
Met956
Lys908
Glu957
Asp1021
Leu959
Mg2+
H2O
Glu966
Arg1007

Tofacitinib

First in class

Pfizer compoud library (~400000 compounds, ca.1996) was screened against the JAK3 catalytic domain

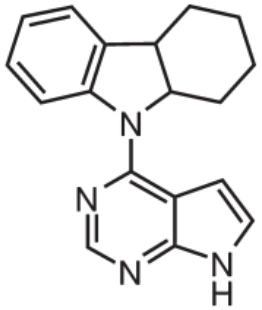

CP-352,664 (210 nM vs JAK3)

SAR

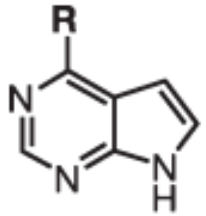

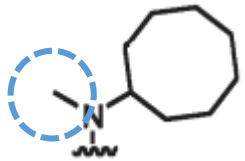

IC50 58 nM

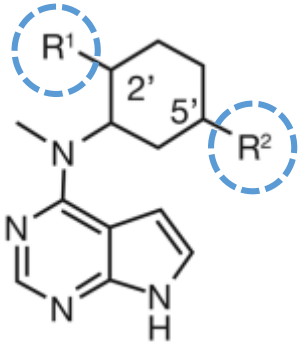

R1=R2=Me

IC50 20 nM

Tofacitinib

First in class

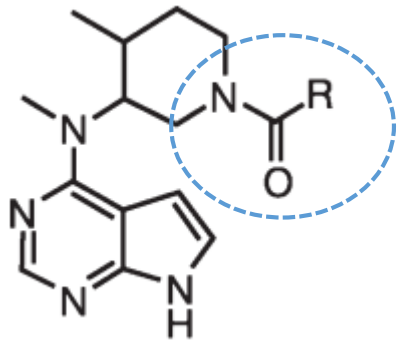

PK issues

↓

polar features to decrease lipophilicity (logP≤2)

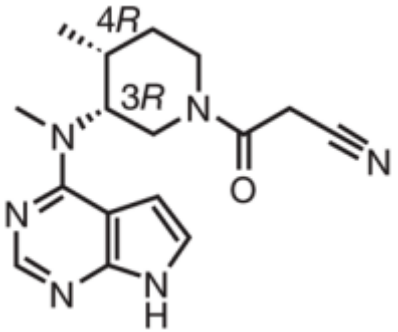

Tofacitinib
CP-690550
JAK3 IC50 = 1nM

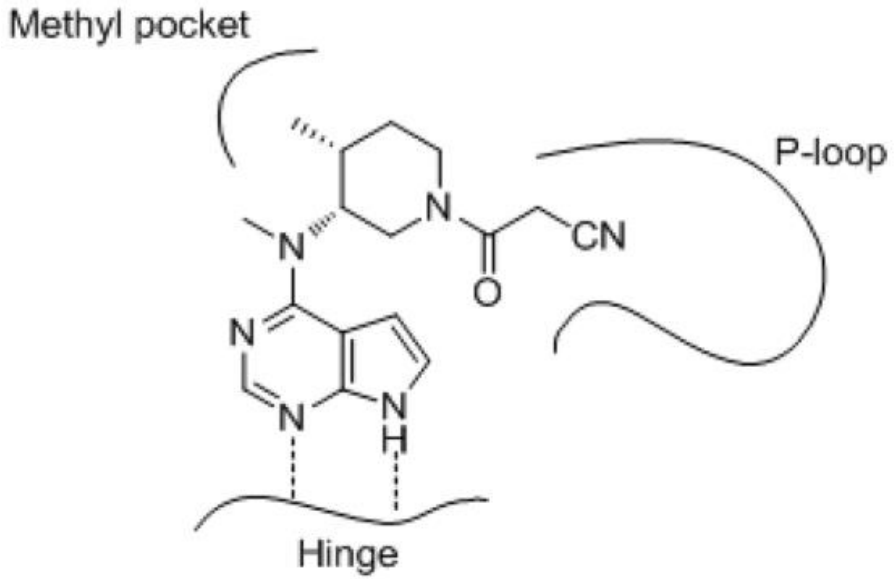

Tofacitinib

First in class

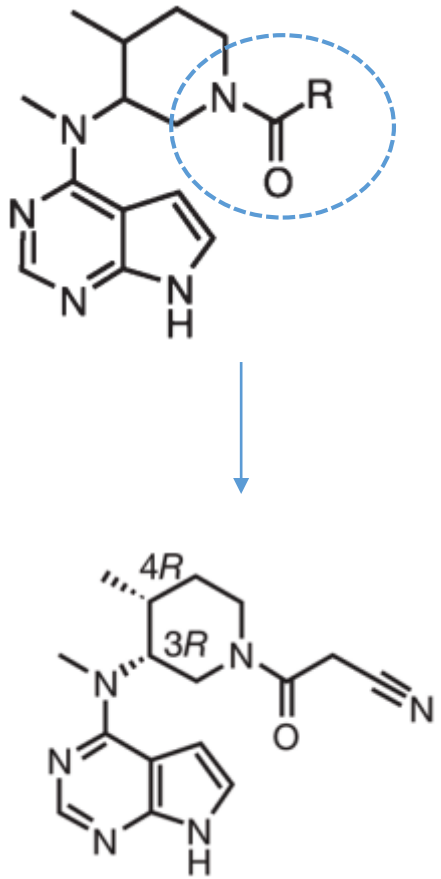

PK issues

↓

polar features to decrease lipophilicity (logP≤2)

Tofacitinib
CP-690550
JAK3 IC50 = 1nM

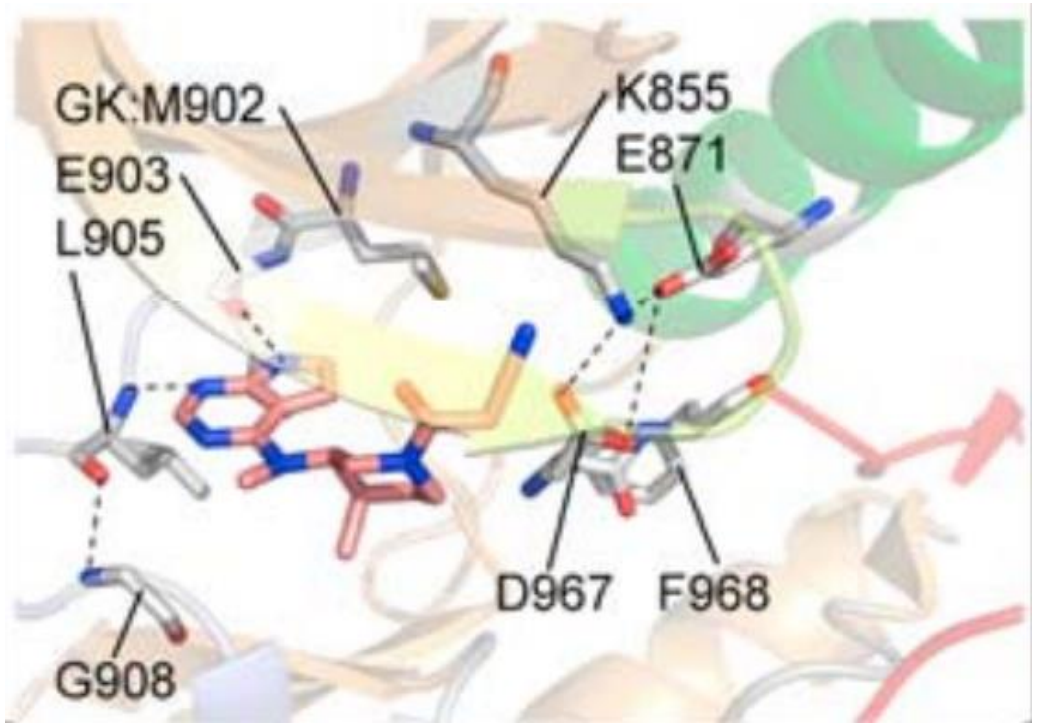

Tofacitinib: PAN-JAK inhibitor

- Reduction of hemoglobin observed in patients
- IC50 (JAK1)=3,2 nM
  IC50 (JAK2)=4,1 nM
  IC50 (JAK3)=1,6 nM
  IC50 (TYK2)=34,0 nM

Interference with Erythropoietin receptor and Thrombopoietin receptor

First in class

Tofacitinib: PAN-JAK inhibitor

- Reduction of hemoglobin observed in patients
- IC50 (JAK1)=3,2 nM
  IC50 (JAK2)=4,1 nM
  IC50 (JAK3)=1,6 nM
  IC50 (TYK2)=34,0 nM

Interference with Erythropoietin receptor and Thrombopoietin receptor

First in class

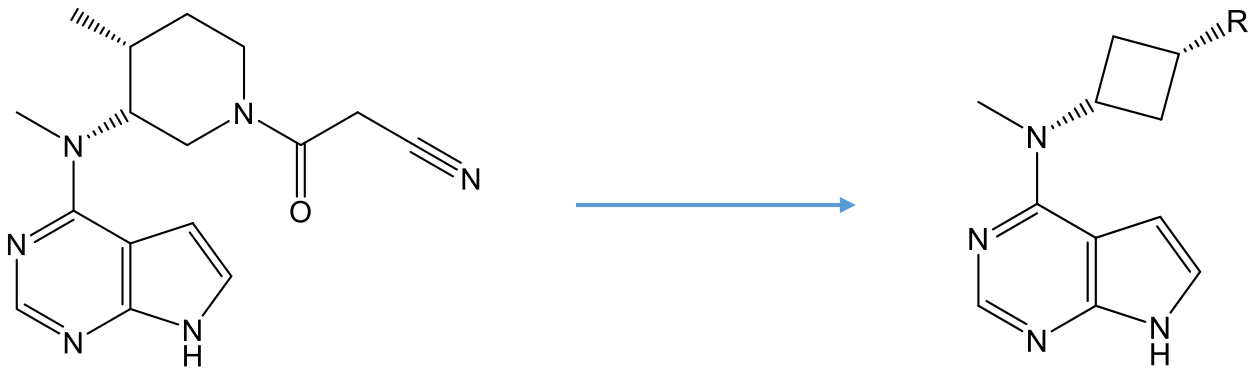

SBDD optimization for Abrocitinib

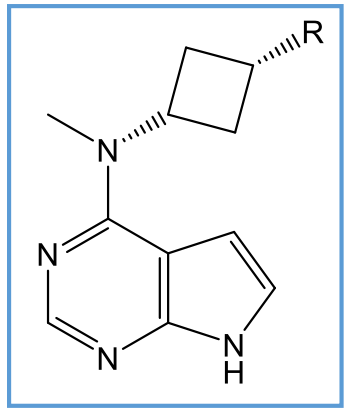

Abrocitinib

Sulfamides

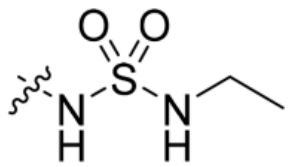

11

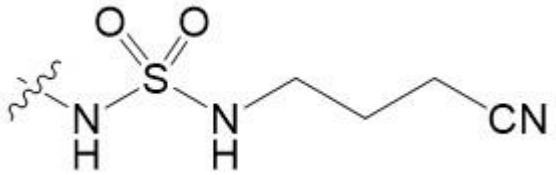

15

Sulfones

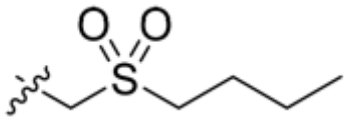

19

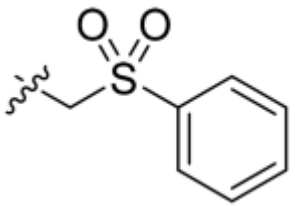

20

Sulfonamides and 'Reverse Sulfonamides'

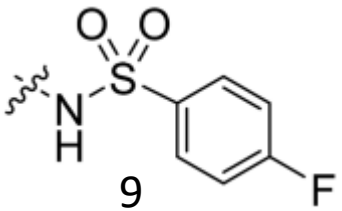

9

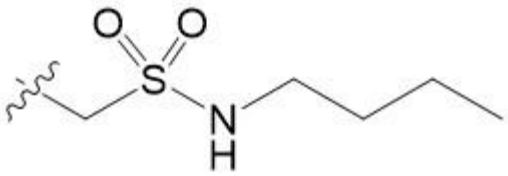

23

Abrocitinib

Abrocitinib

Results:

- Selectivity generally improved as the side chains grew larger
- Sulfamide subset is of lower interest (poorest JAK1 potency)
- Sulfonamides achieve the best selectivity for JAK1
- Enhanced metabolic stability when log $D_{7.4}$<2.0

IC50(JAK1)= 29 nM
IC50(JAK2)= 803 nM
IC50(JAK3)= >10,000 nM
IC50(TYK2)= 1250 nM
logD=1.9

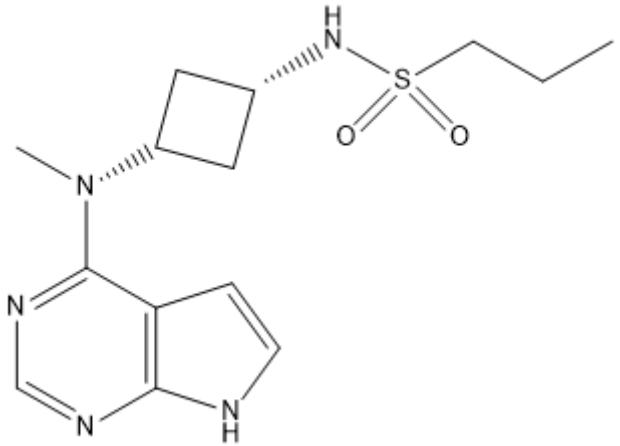

PF-04965842

Abrocitinib

Results:

- Selectivity generally improved as the side chains grew larger
- Sulfamide subset is of lower interest (poorest JAK1 potency)
- Sulfonamides achieve the best selectivity for JAK1
- Enhanced metabolic stability when log $D_{7.4}$<2.0

Abrocitinib

IC50(JAK1)= 29 nM
IC50(JAK2)= 803 nM
IC50(JAK3)= >10,000 nM
IC50(TYK2)= 1250 nM
logD=1.9

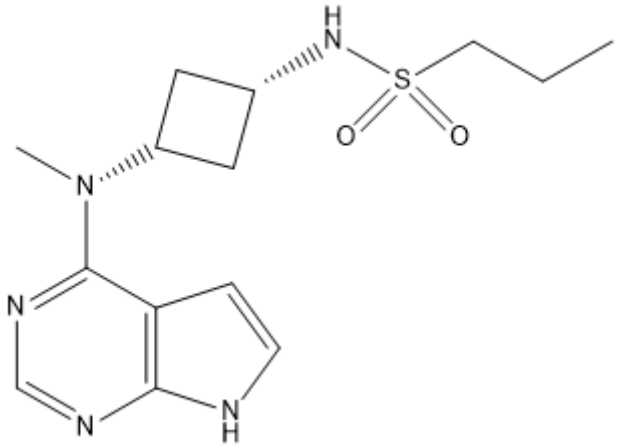

PF-04965842

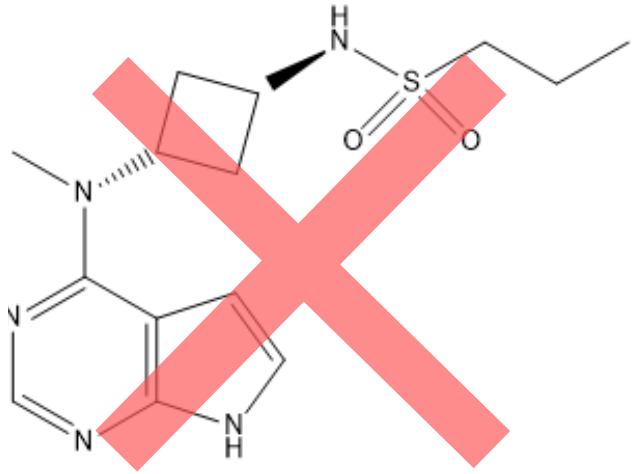

Understanding JAK1/JAK2 selectivity

The residue differences (within 5 Å radius from the ligand) are located in the hinge region, phosphate-binding region, (i.e., P-loop) and in the solvent exposed regions toward the periphery of the binding site.

Abrocitinib

location in the kinase domain	JAK1	JAK2
hinge	Phe958	Tyr931
hinge	Ser961	Tyr934
hinge	Lys965	Arg938
hinge	Glu966	Asp939
P-loop	Glu883	Lys857
P-loop	His885	Asn859
P-loop	Lys888	Ser862

Understanding JAK1/JAK2 selectivity

Although the JAK1 kinase domain shares only 53% overall sequence identity with JAK2, most of the residues in the ATP-binding site are conserved between the two enzymes.

Abrocitinib

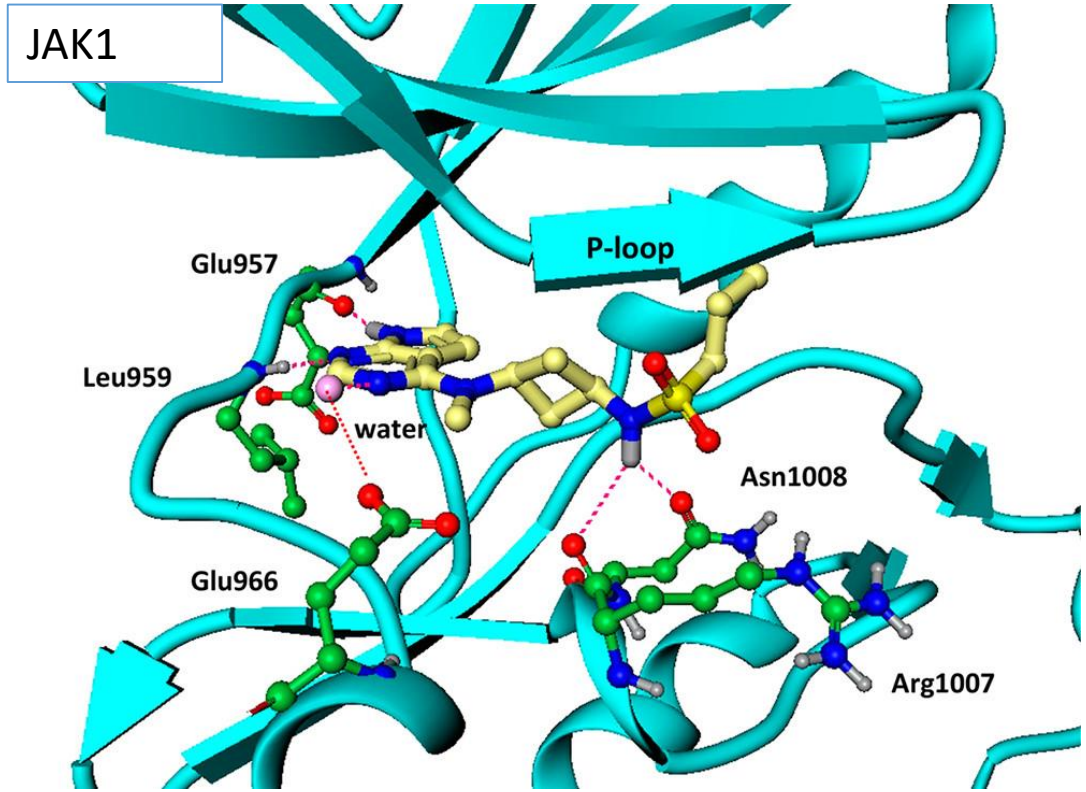

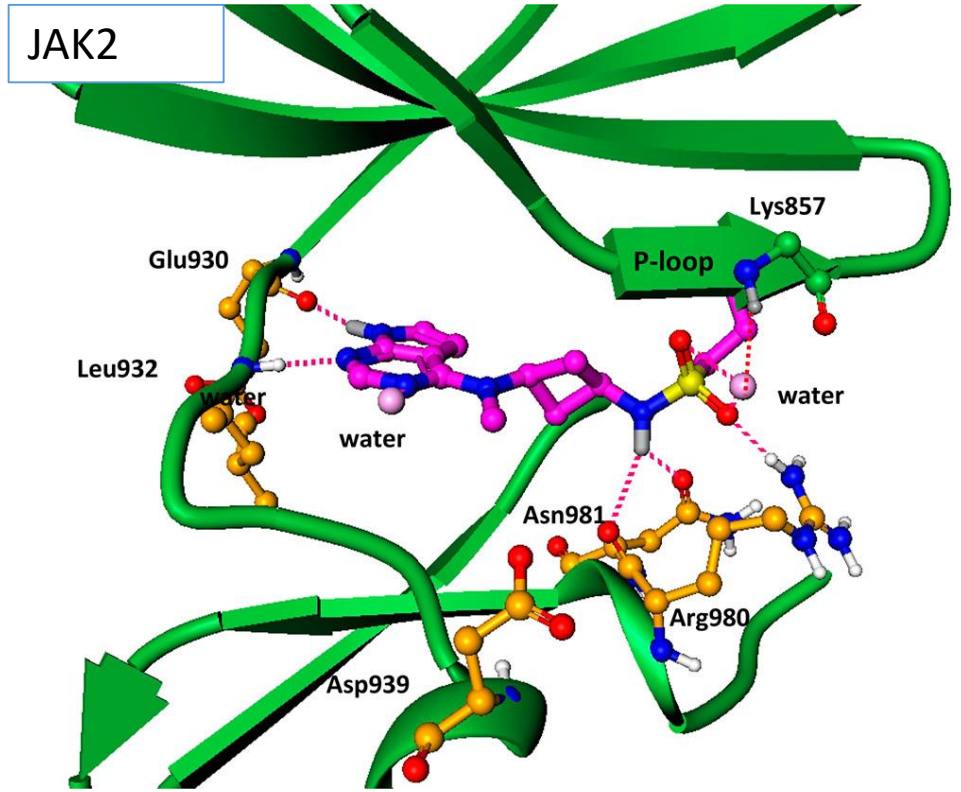

Understanding JAK1/JAK2 selectivity

Although the JAK1 kinase domain shares only 53% overall sequence identity with JAK2, most of the residues in the ATP-binding site are conserved between the two enzymes.

Abrocitinib

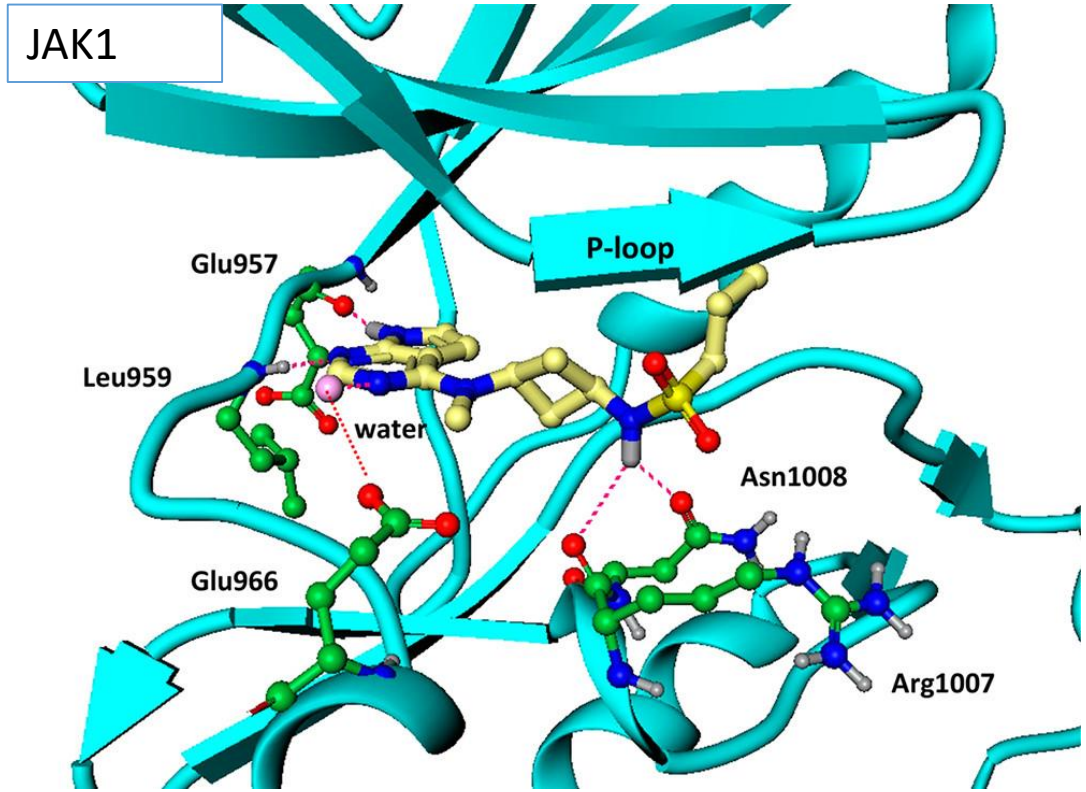

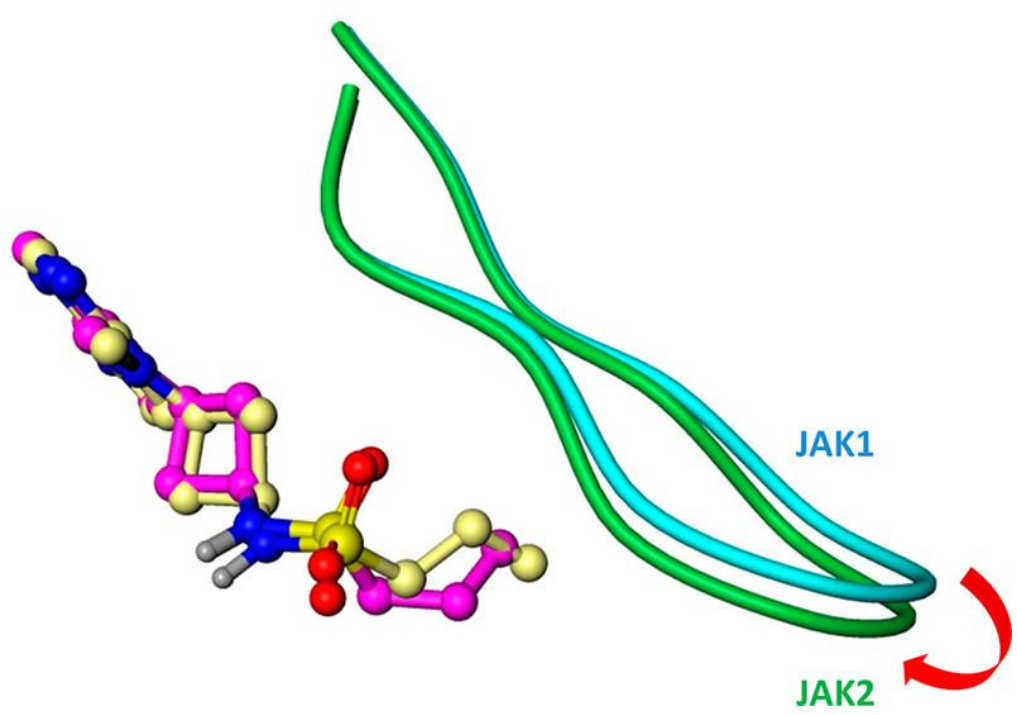

Phase I

Abrocitinib

- 79 Healthy subjects, adults, randomized in a 3:1 ratio of Abrocitinib:placebo

Most frequent treatment-emergent adverse events:

- Headache (*n*=13)
- Diarrhoea (*n*=11)
- Nausea (*n*=11)

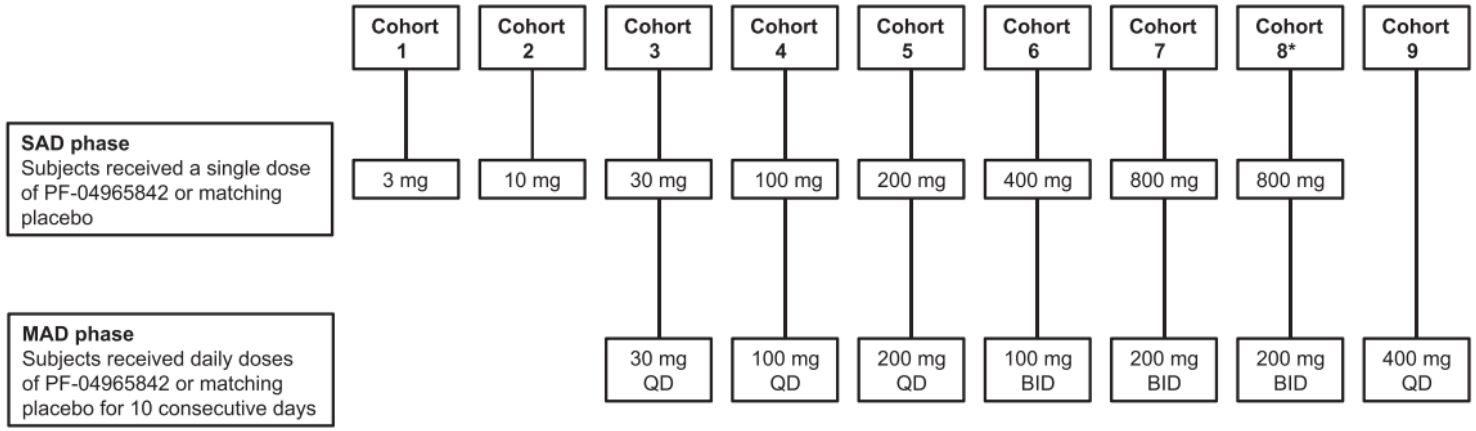

Phase I

Abrocitinib

- 79 Healthy subjects, adults, randomized in a 3:1 ratio of Abrocitinib:placebo

Most frequent treatment-emergent adverse events:

- Headache (*n*=13)
- Diarrhoea (*n*=11)
- Nausea (*n*=11)

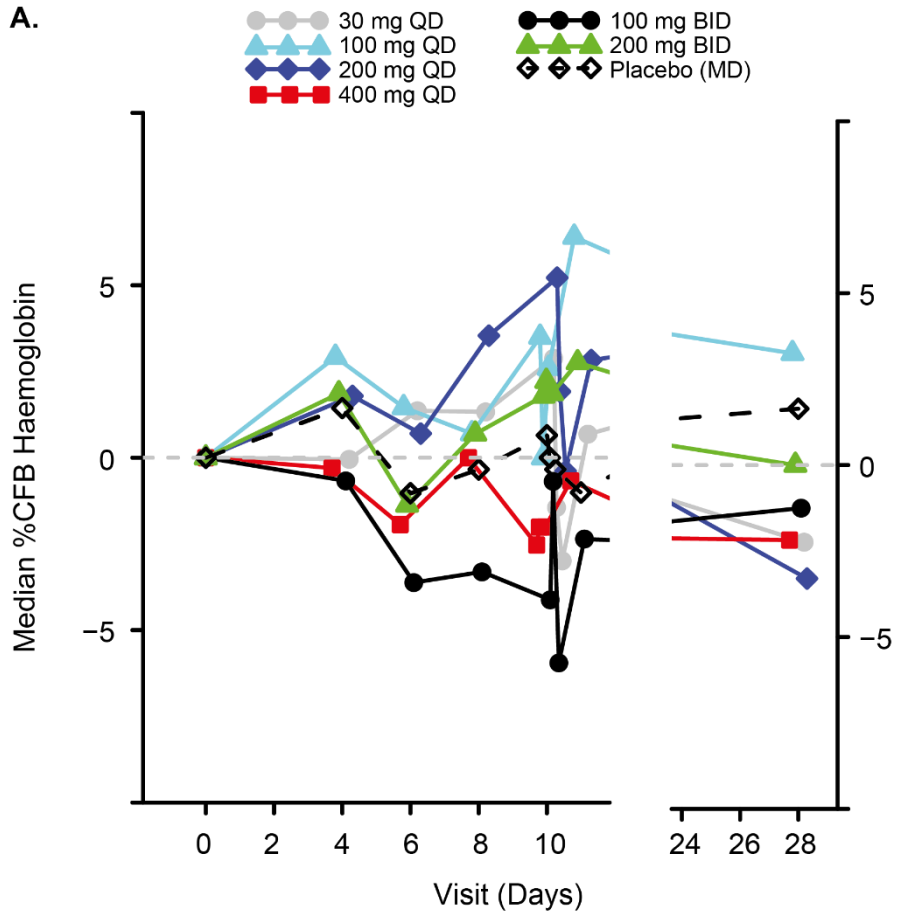

Phase I

Abrocitinib

SAD

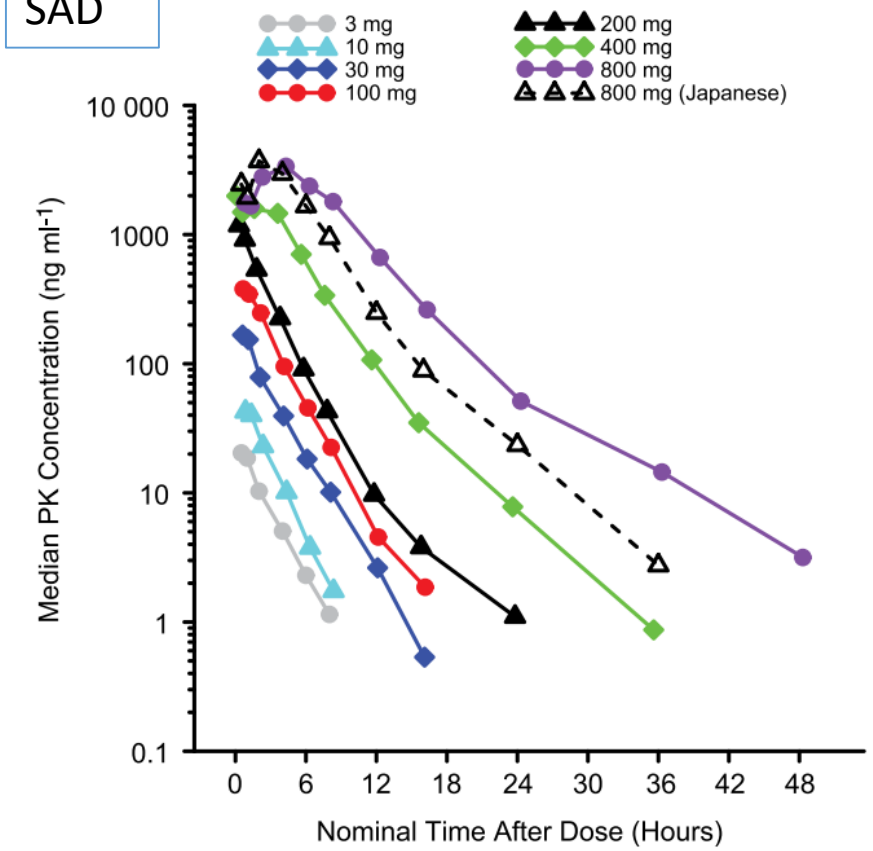

MAD

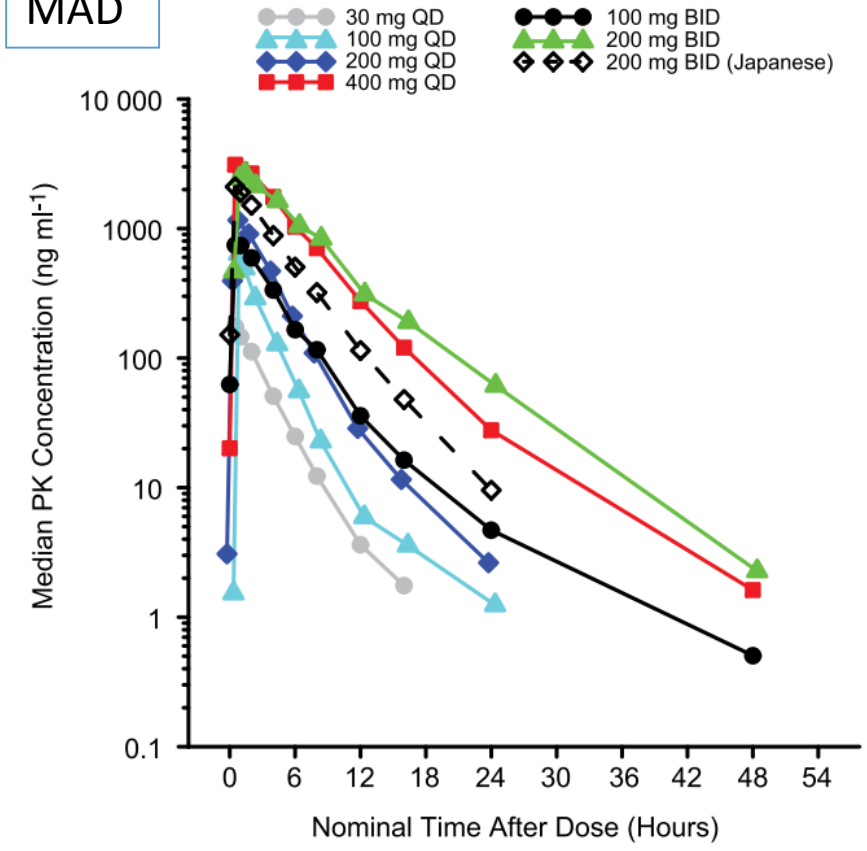

Phase II

- 267 partecipants (adults) randomly assigned 1:1:1:1:1 to receive Abrocitinib (200 mg, 100 mg, 30 mg, or 10 mg) or placebo for 12 weeks

Abrocitinib

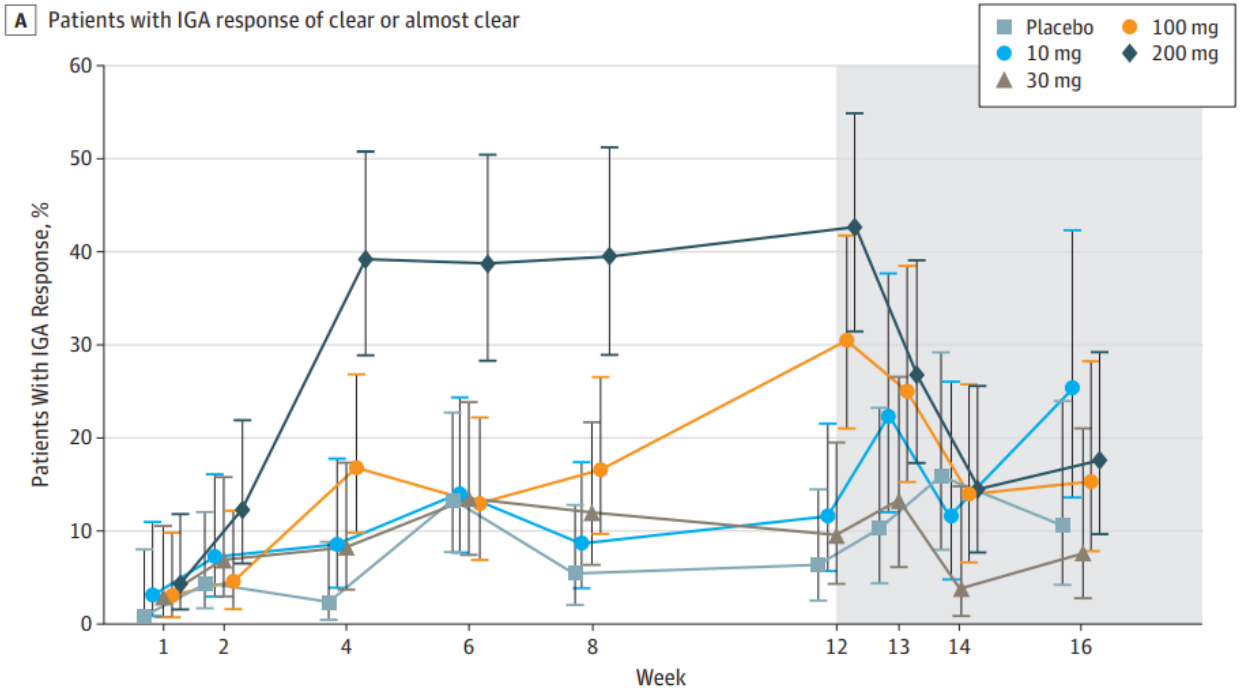

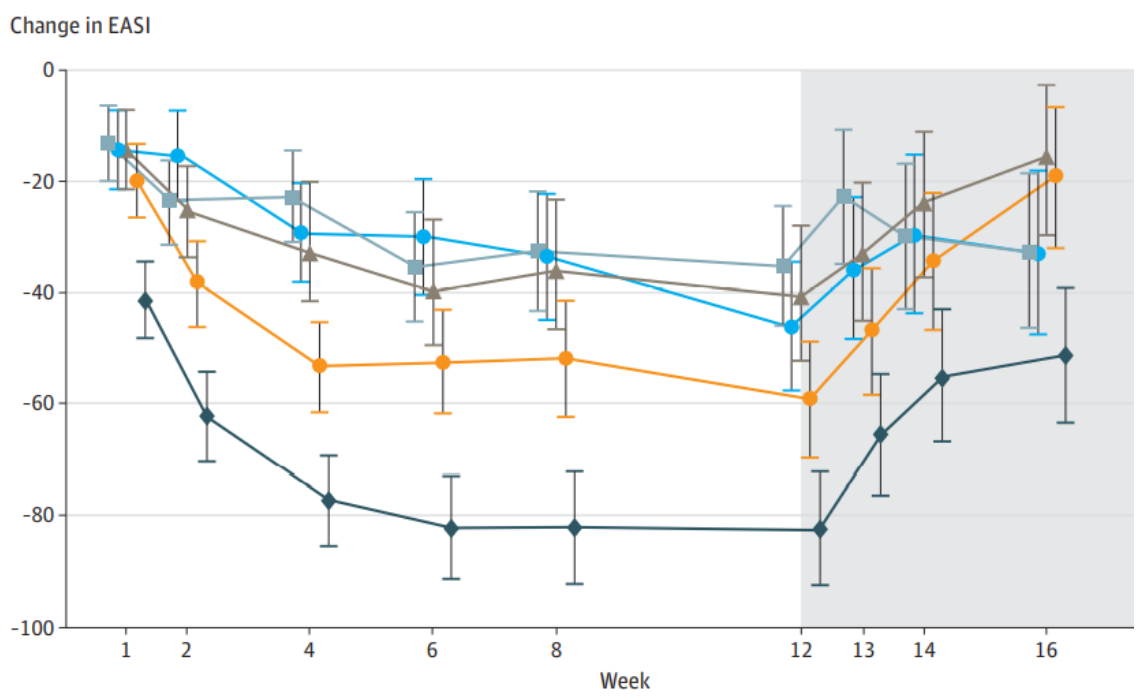

Phase II

Abrocitinib

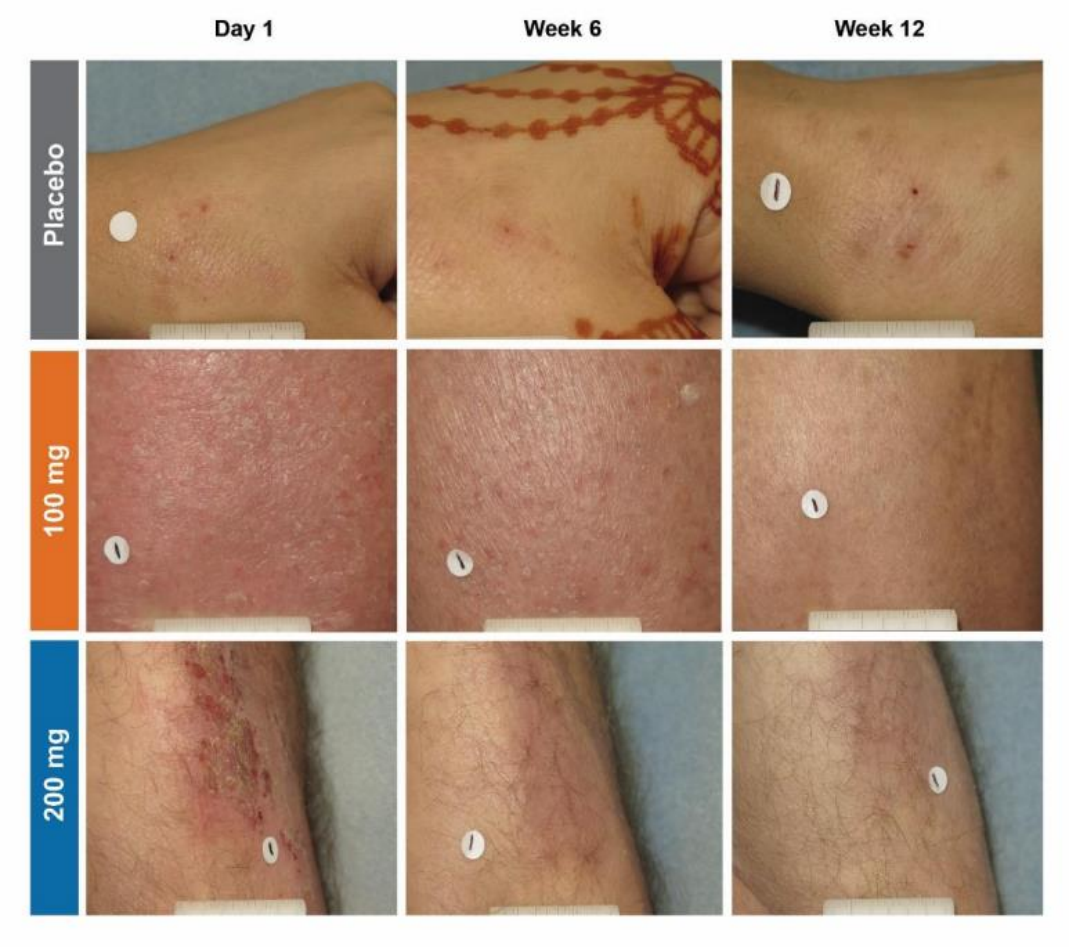

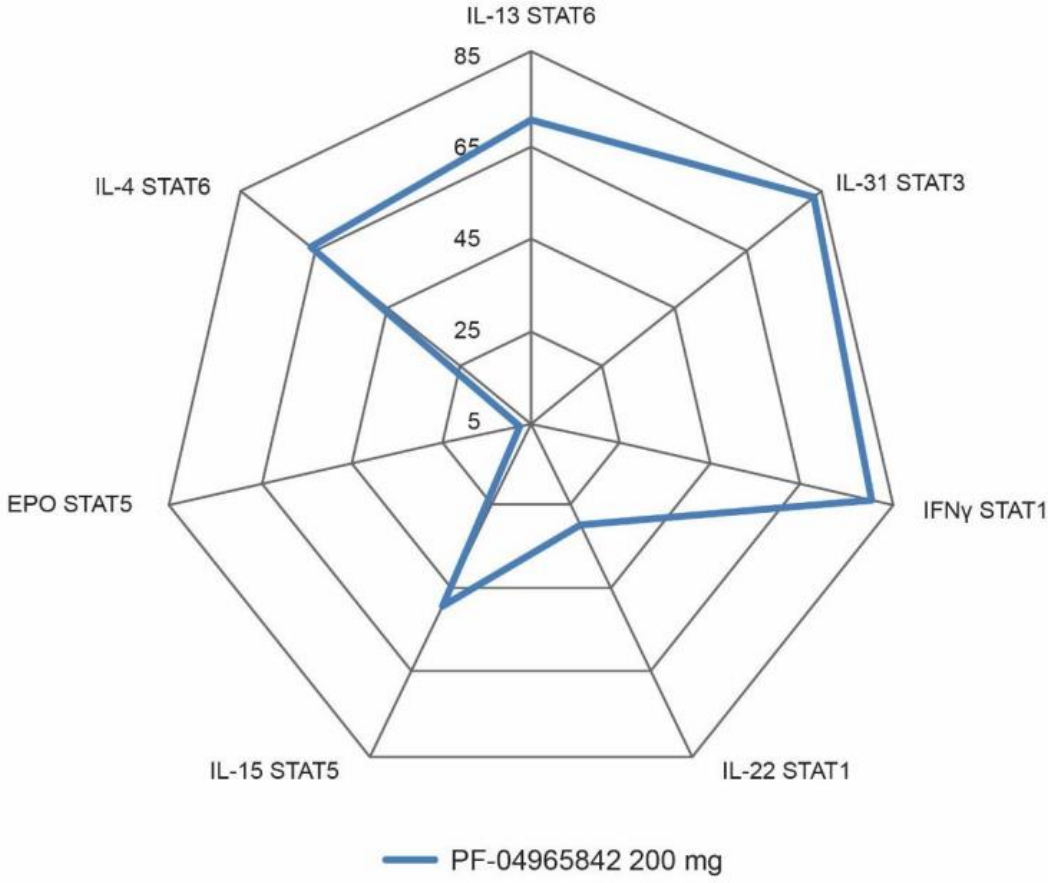

Phase III

- 391 partecipants (adolescents ≥12 and adults) randomly assigned 2:2:1 to receive once-daily Abrocitinib in 200mg or 100mg doses or placebo

Abrocitinib

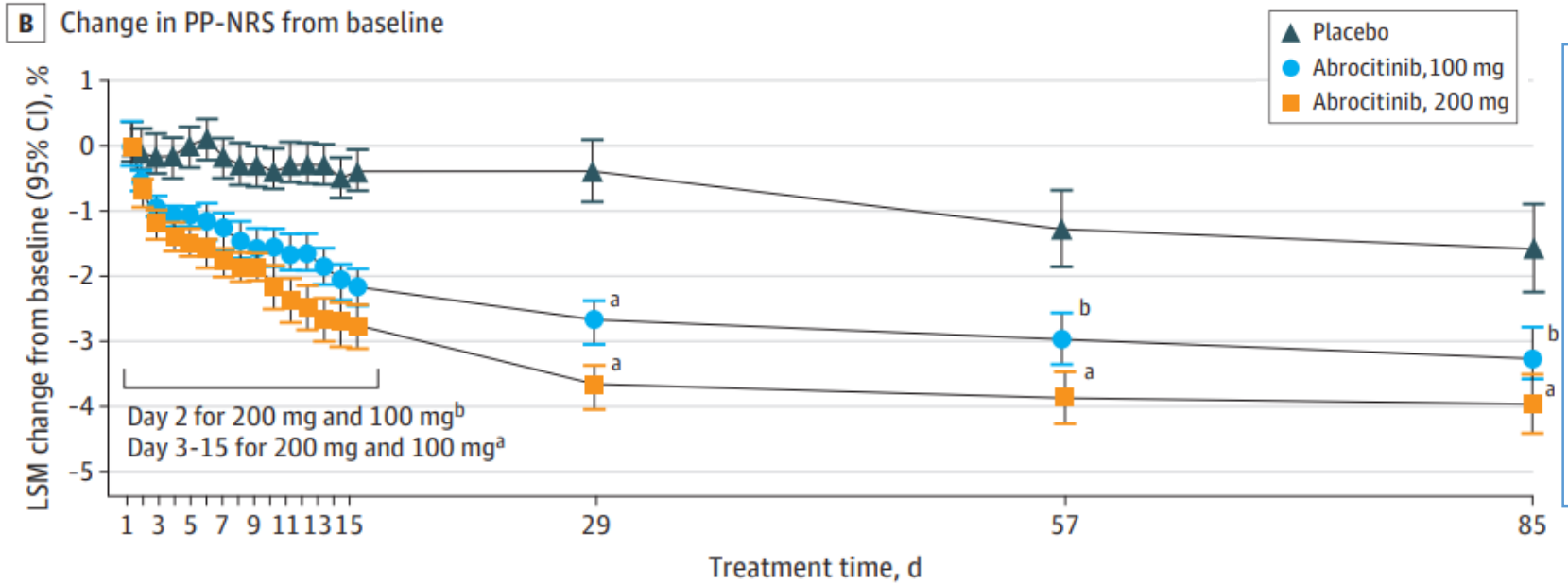

Percentage of patients achieving the desired score

	100 mg	200 mg
IGA	28,4%	38,1%
EASI	44,5%	61,0%
PP-NRS	45,2%	55,3%

Toxicity and metabolism

- No deaths, no serious adverse events → Nonclinical toxicology
- CYP450-family mediated metabolism:

Abrocitinib

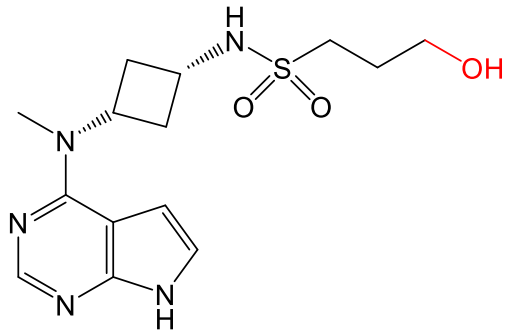

M1

Less active

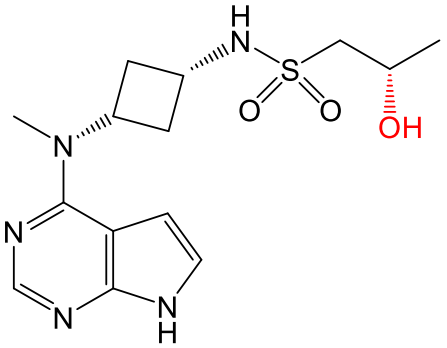

M2

Comparable activity

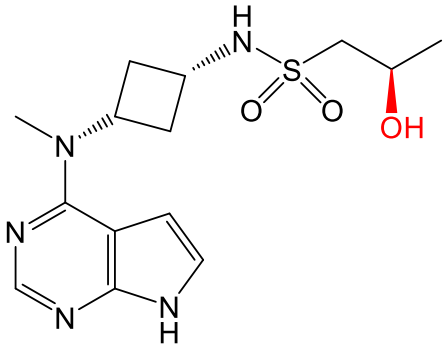

M3

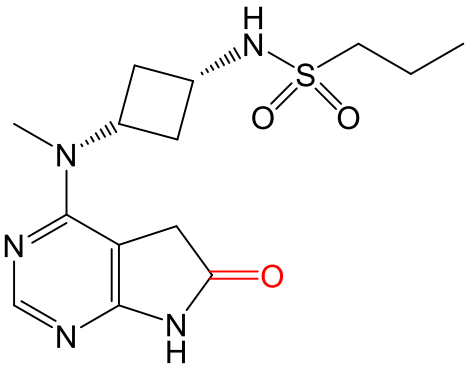

M4

Conclusions

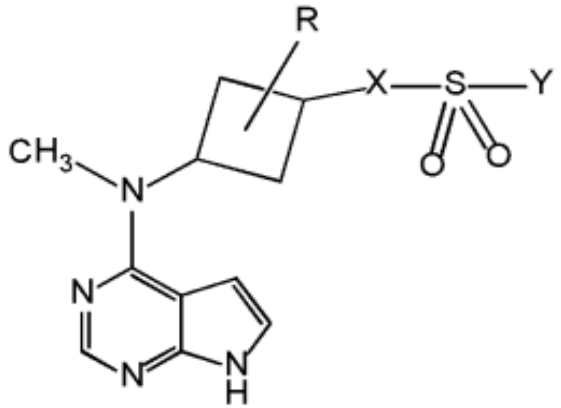

- JAK1 inhibitor with 28-fold selectivity over JAK2, >340-fold over JAK3, 43-fold over TYK2 as well as the broader kinome
- 30-40% of patients treated with Abrocitinib show desired improvement in key-index for Atopic Dermatitis
- Focus on the long-term efficacy and safety

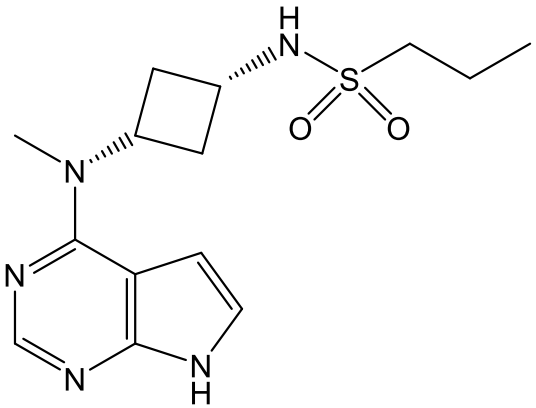

Bibliography

Doi:10.3390/microorganisms8111743
https://doi.org/10.1038/s41392-021-00791-1
http://dx.doi.org/doi:10.1016/j.phrs.2015.10.021
Doi: 10.1021/jm1004286
http://dx.doi.org/10.1021/acs.jmedchem.7b01598
Doi:10.1111/bcp.13612
Doi:10.1001/jamadermatol.2019.2855
Doi:10.1001/jamadermatol.2020.1406

Journal of Medicinal Chemistry

Article

pubs.acs.org/jmc

Discovery of (*R*,*E*)-*N*-(7-Chloro-1-(1-[4-(dimethylamino)but-2-enoyl]azepan-3-yl)-1*H*-benzo[*d*]imidazol-2-yl)-2-methylisonicotinamide (EGF816), a Novel, Potent, and WT Sparing Covalent Inhibitor of Oncogenic (L858R, ex19del) and Resistant (T790M) EGFR Mutants for the Treatment of EGFR Mutant Non-Small-Cell Lung Cancers

Gérald Lelais,[*,†] Robert Epple,[†] Thomas H. Marsilje,[†] Yun O. Long,[†] Matthew McNeill,[†] Bei Chen,[†] Wenshuo Lu,[†] Jaganmohan Anumolu,[‡] Sangamesh Badiger,[§] Badry Bursulaya,[†] Michael DiDonato,[†] Rina Fong,[†,∥] Jose Juarez,[†] Jie Li,[†] Mari Manuia,[†] Daniel E. Mason,[†] Perry Gordon,[†] Todd Groessl,[†] Kevin Johnson,[†] Yong Jia,[†] Shailaja Kasibhatla,[†] Chun Li,[†] John Isbell,[†] Glen Spraggon,[†] Steven Bender,[†] and Pierre-Yves Michellys[†]

A.A. 2022/23

Lorenzo Taglietti

Non-Small-Cell Lung Cancer (NSCLC)

NSCLC causes abnormal cells growth in the lungs to reproduce rapidly and out of control

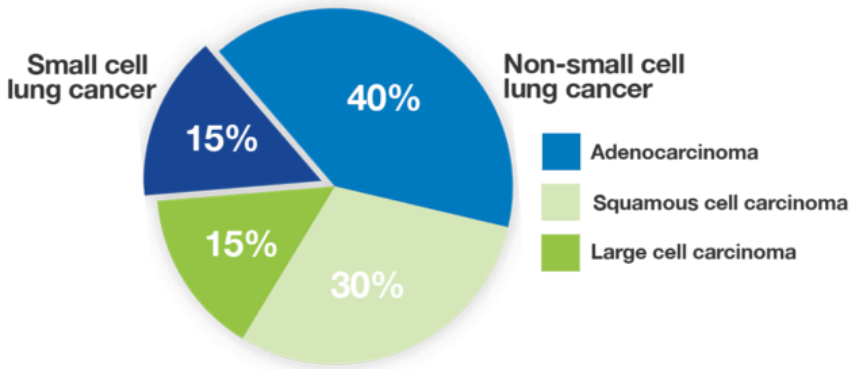

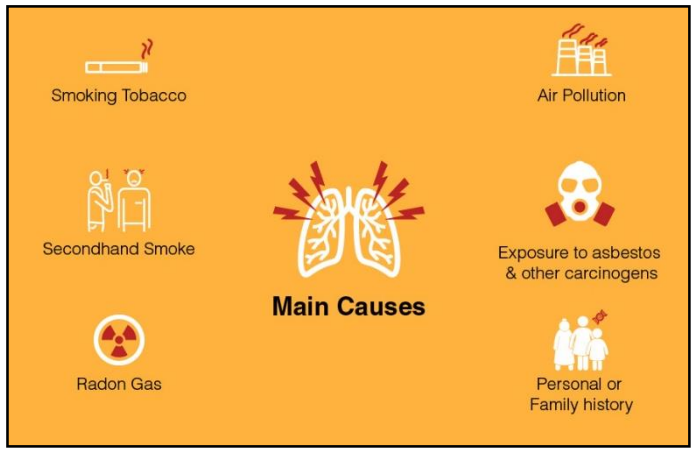

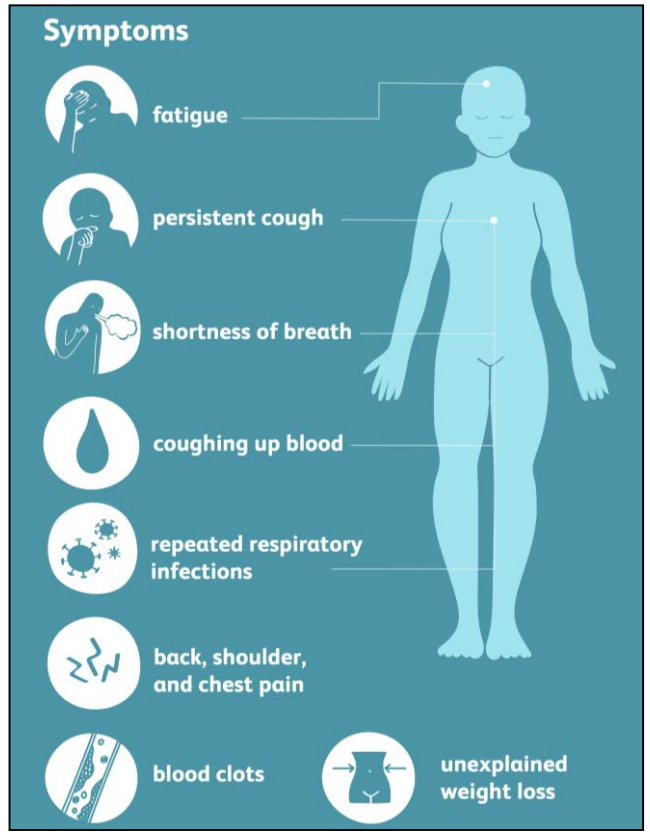

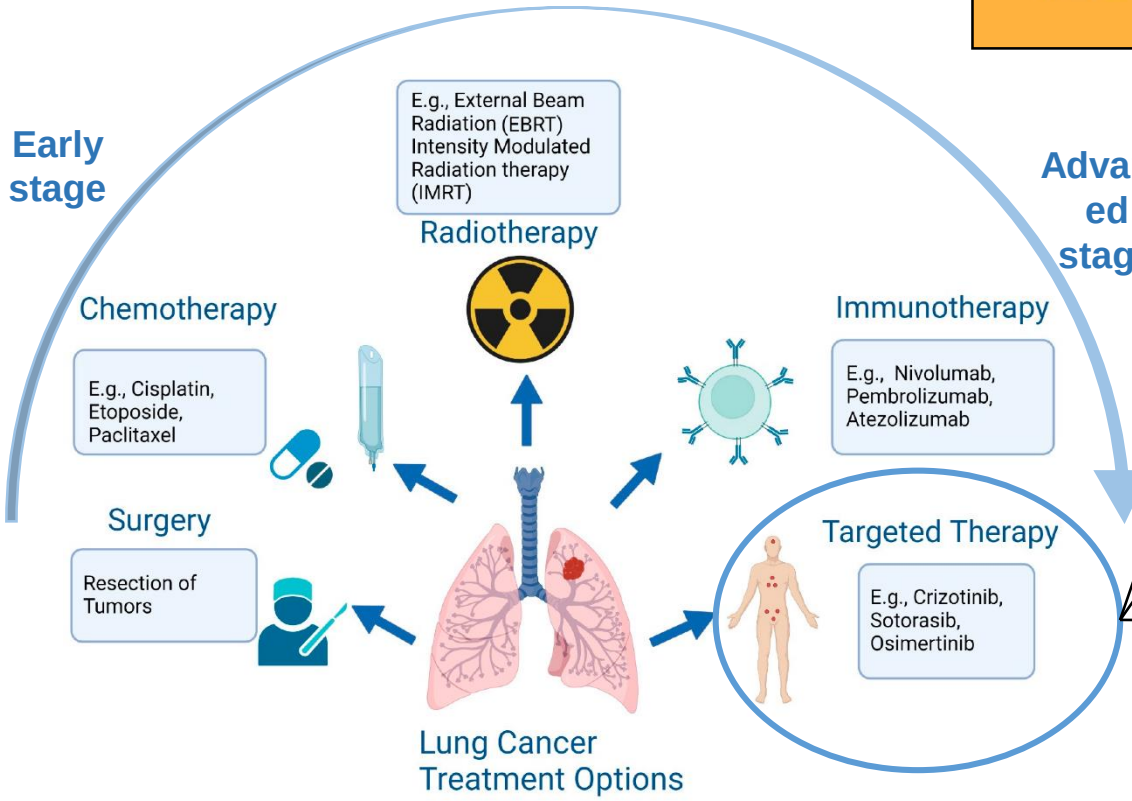

BRAF, HER2/neu, KRAS, c-Met and others

Anaplastic Lymphoma Kinase (ALK)

Epidermal Growth Factor Receptor (EGFR)

EGFR inhibitors (TKIs)

NSCLC – EGFR: structure and function

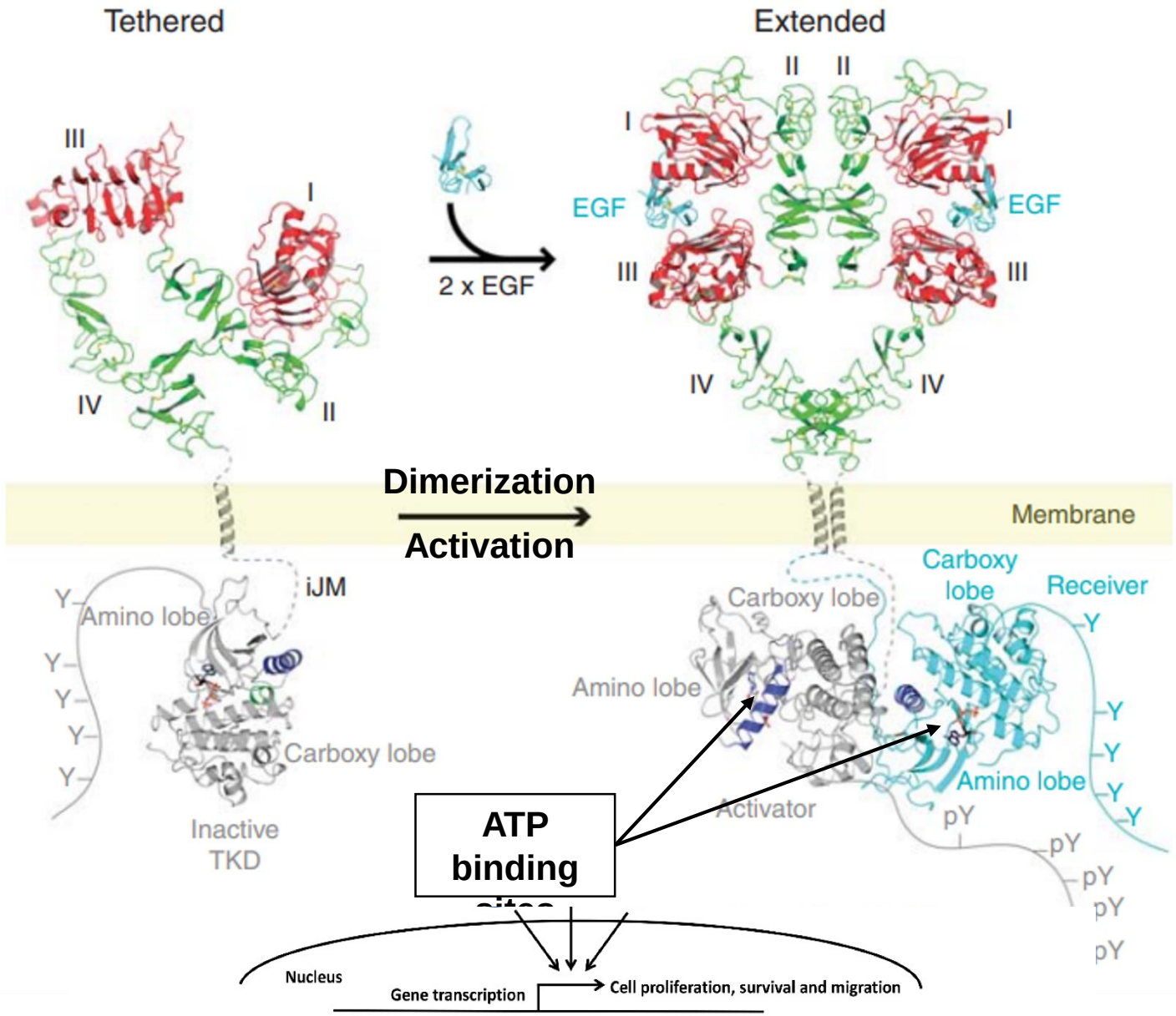

Extracellular domain: «receptor mediated» dimerization mechanism	EGF binding induces conformational changes that lead to activation
Intracellular domain: «activator» and «receiver» dimerization mechanism	Autophosphorilation and kinase domain activation

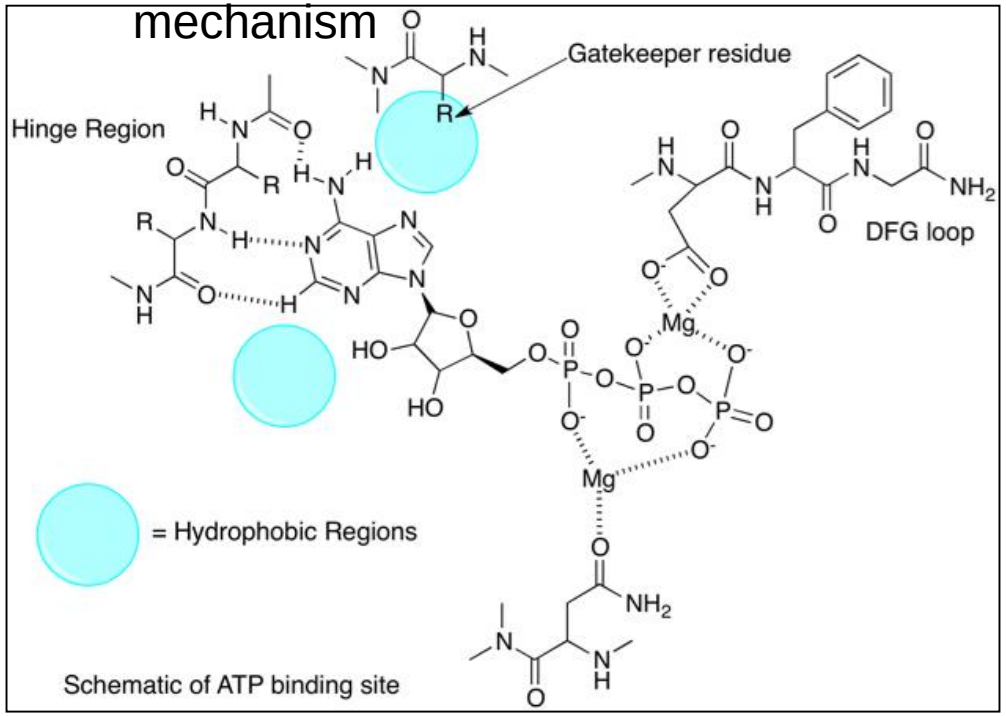

NSCLC – EGFR: pathology outlines

- EGFR overexpression → EGFR overactivation
- L858R mutation
- Exon 19 deletion → Ligand independent EGFR activation

→ **Oncogenic**

- T790M mutation → **Drug resistant**

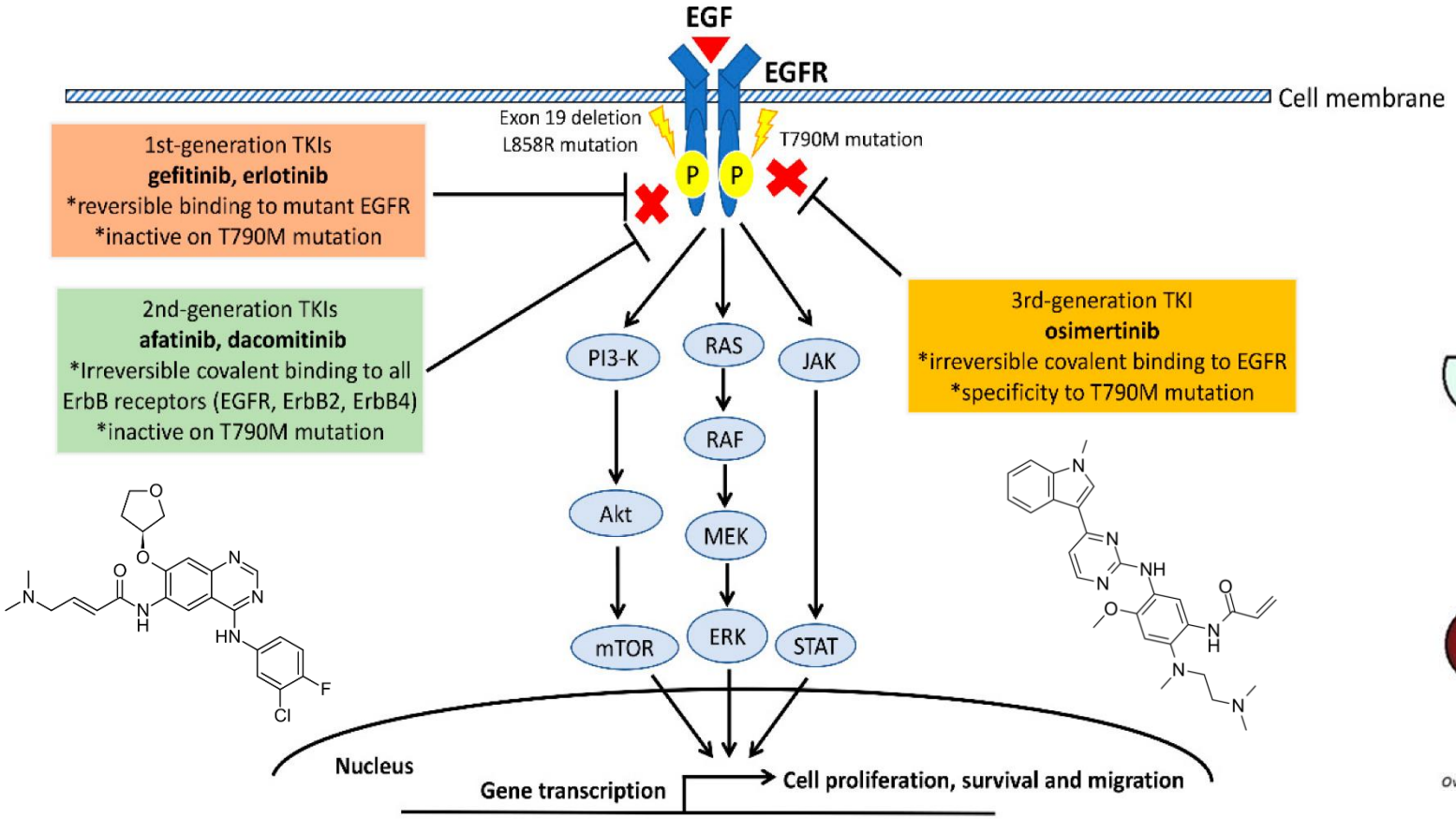

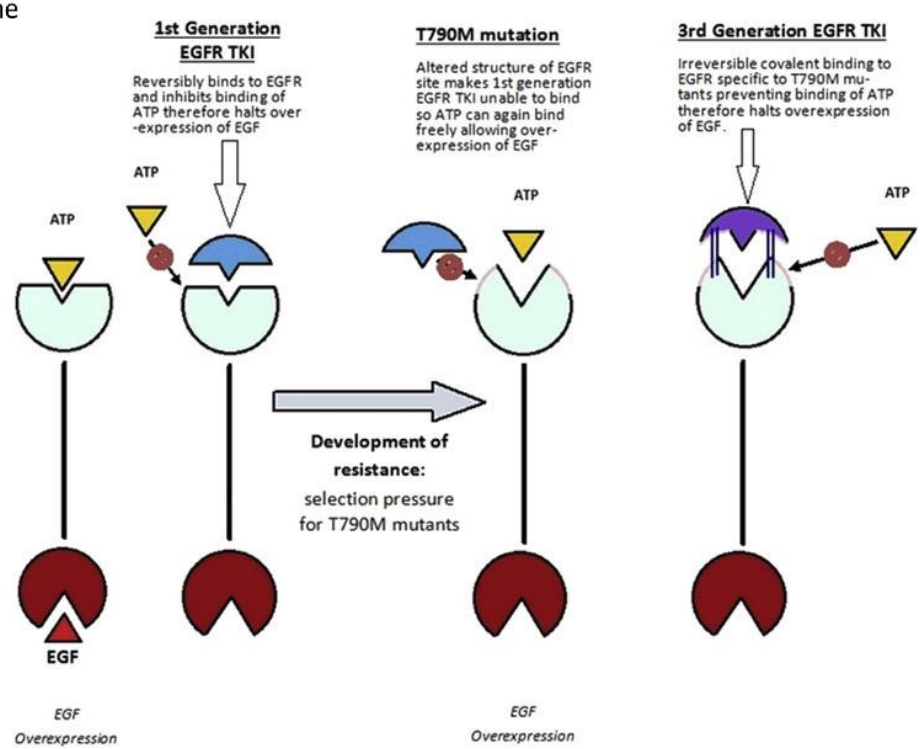

NSCLC – EGFR: T790M mutation

Substitution of Threonine 790 with Methionine (T790M)

- After 10-16 months of treatment with 1st and 2nd generation TKIs emerges drug resistance in patients
- In 50% of cases drug resistance is due to T790M mutation at the gatekeeper position

Affinity for the drug decreases

↓

No displacement of ATP

↓

Drug resistance

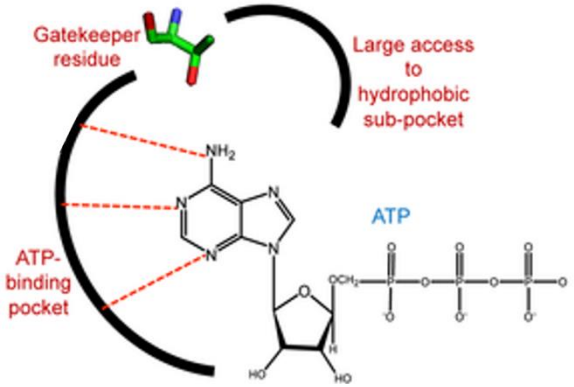

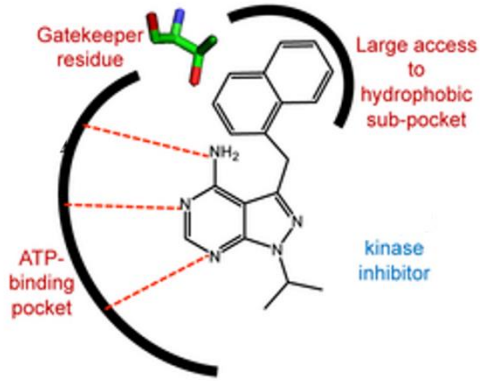

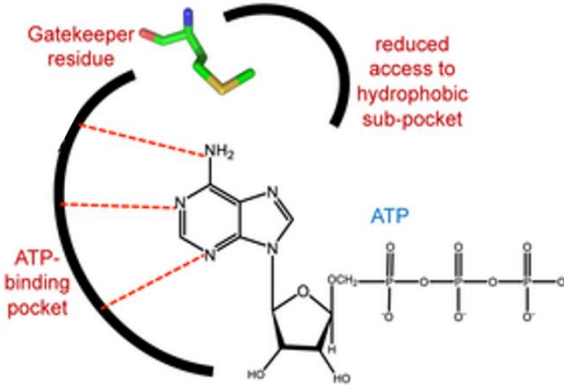

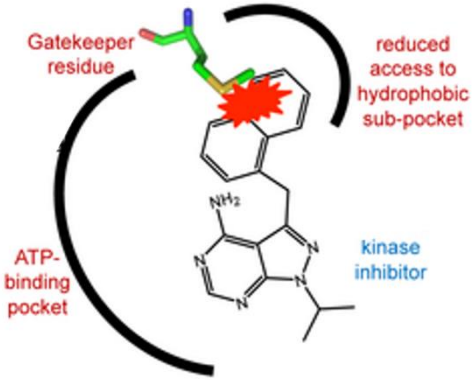

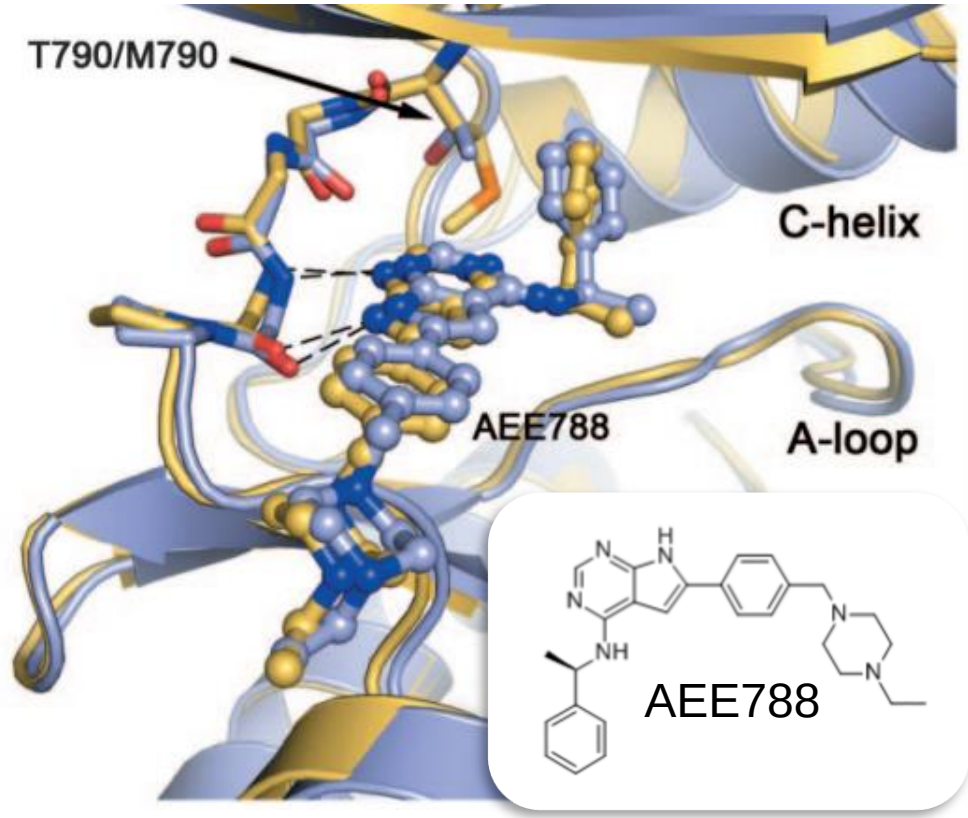

Design of EGF816 – HTS hit

EGFR [L858R-T790M] kinase domain
IC_{50} at 1 μM ATP

⇩ Hit reconfirmation and expansion

EGFR [L858R-T790M] kinase domain
EGFR [L858R] kinase domain
EGFR [WT] kinase domain
IC_{50} at low (μM) and high (mM) ATP

⇩ ⇨ allosteric hits

ATP-competitive hit:

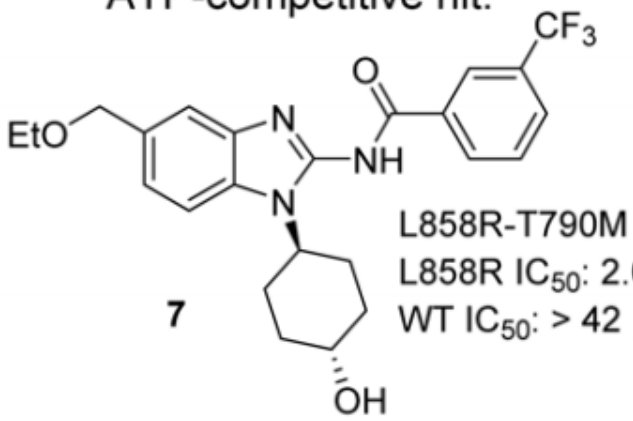

7

L858R-T790M IC_{50}: 0.47 ± 0.07 μM
L858R IC_{50}: 2.08 ± 0.86 μM
WT IC_{50}: > 42 μM

Unique structural motif in the EGFR field

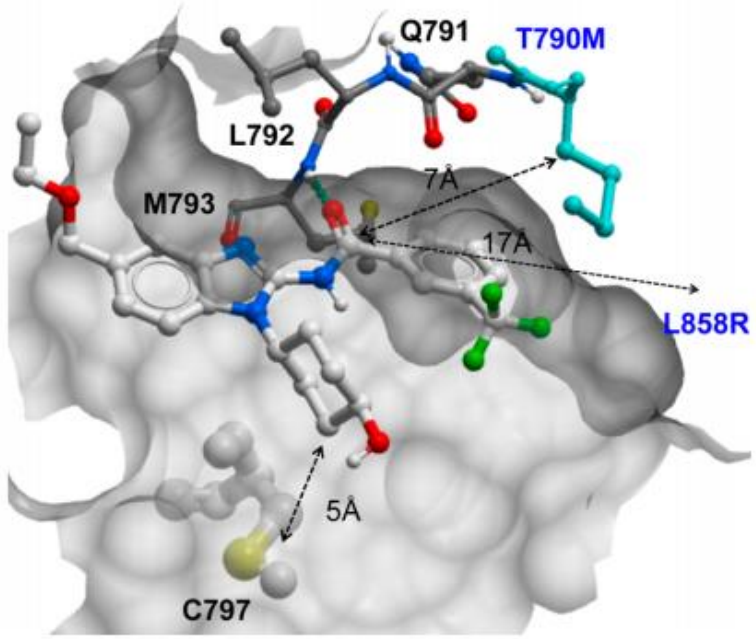

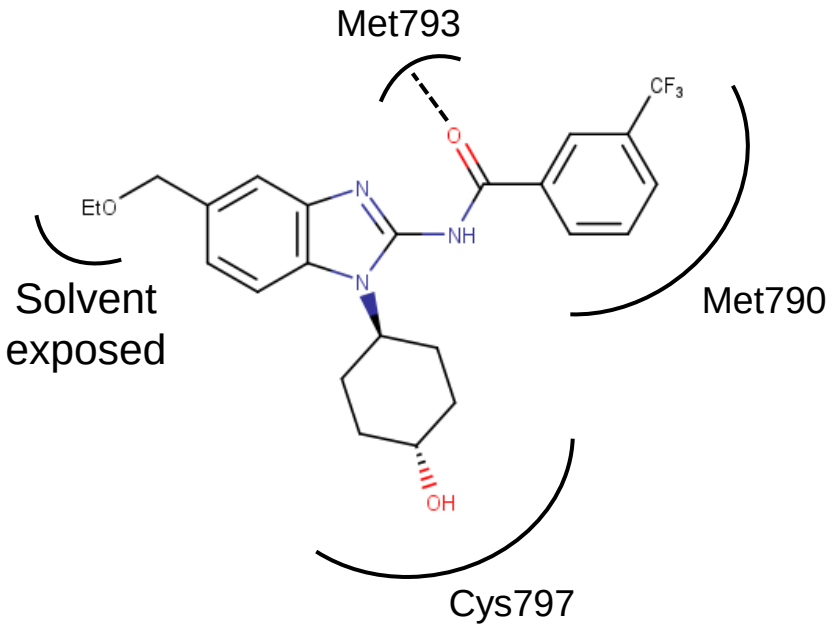

ATP-competitive hit

⇩

Targeted covalent inhibitors

⇩

Selectivity | **Pharmacodynamics** | **Potency**

Design of EGF816 – From hit to lead

Benzimidazole core

R = OEt is solvent exposed → Lack of stabilizing protein interactions → Rationale for better substitution

compd	R	L858R-T790M	L858R	WT
23	H	0.26 ± 0.07	2.00 ± 0.41	>50
24	4-Me	1.37 ± 0.56	11.75 ± 5.22	>50
25	5-Me	0.14 ± 0.10	>8.48	>11.78
26	6-Me	0.28 ± 0.12	>16	>50
27	7-Me	0.09 ± 0.01	0.68 ± 0.07	5.27 ± 2.42

[a]Biochemical IC_{50} (μM) assessed at 10 μM ATP concentration for either mutants (L858R and L858R-T790M) and WT EGFR constructs. All data are an average of at least duplicate measurements.

☹ 4-Me points towards hinge binding region

☹ H and 6-Me improve IC_{50} for L858R-T790M

😐 5-Me and 7-Me slightly improve potency

☺ 7-Me keeps activity on L858R mutant

Selectivity towards WT EGFR → Add a well-placed Michael acceptor capable of reacting with Cys797

Hinge region

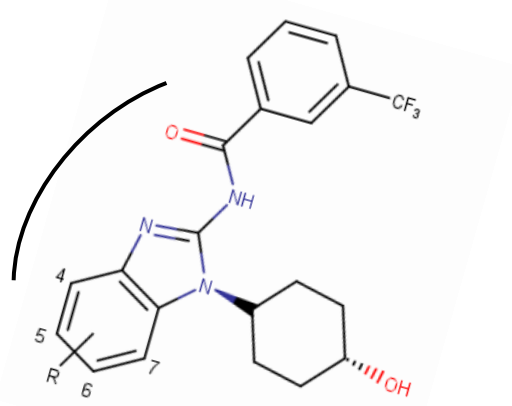

Design of EGF816 – From hit to lead

Linker optimization

- Preincubation with L958R/T790M mutants enzymes with 1mM ATP
- After 90 min of incubation 32g showed IC_{50} < 0.002 µM

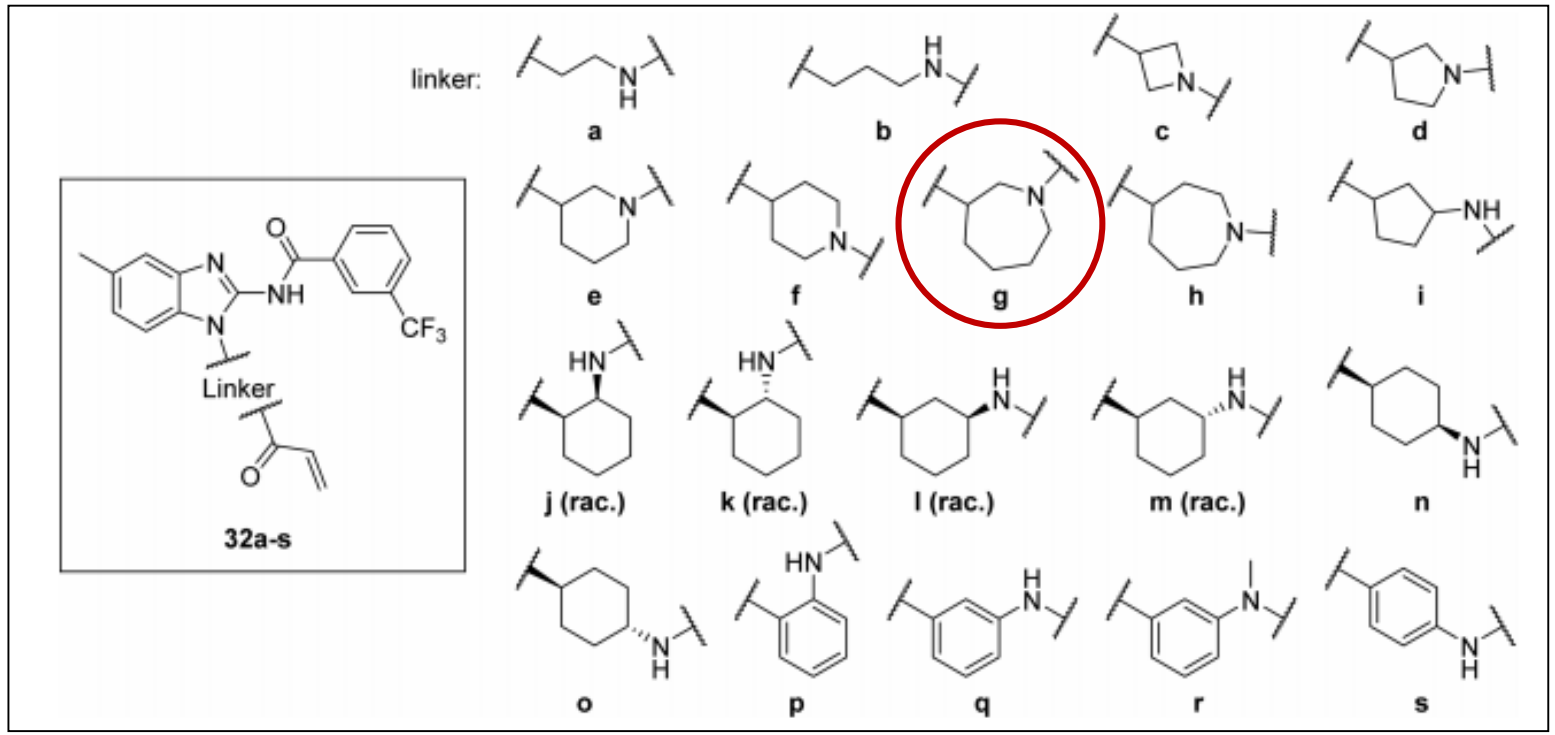

WT IC_{50}: 249.6 nM	L858R IC_{50}: 14.84 nM	L858R-T790M IC_{50}: 1.39 nM

32g is a racemic mixture

↓

(R) eutomer is >200-fold more potent than distomer*(S)*

↓

7-Me derivative is more effective

↓

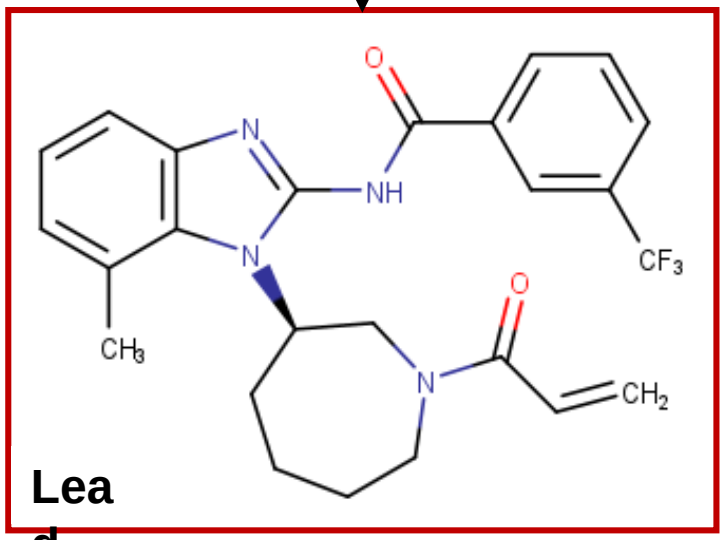

Lead

Design of EGF816 – Lead selectivity and properties

Superposition of WT EGFR and T790M EGFR

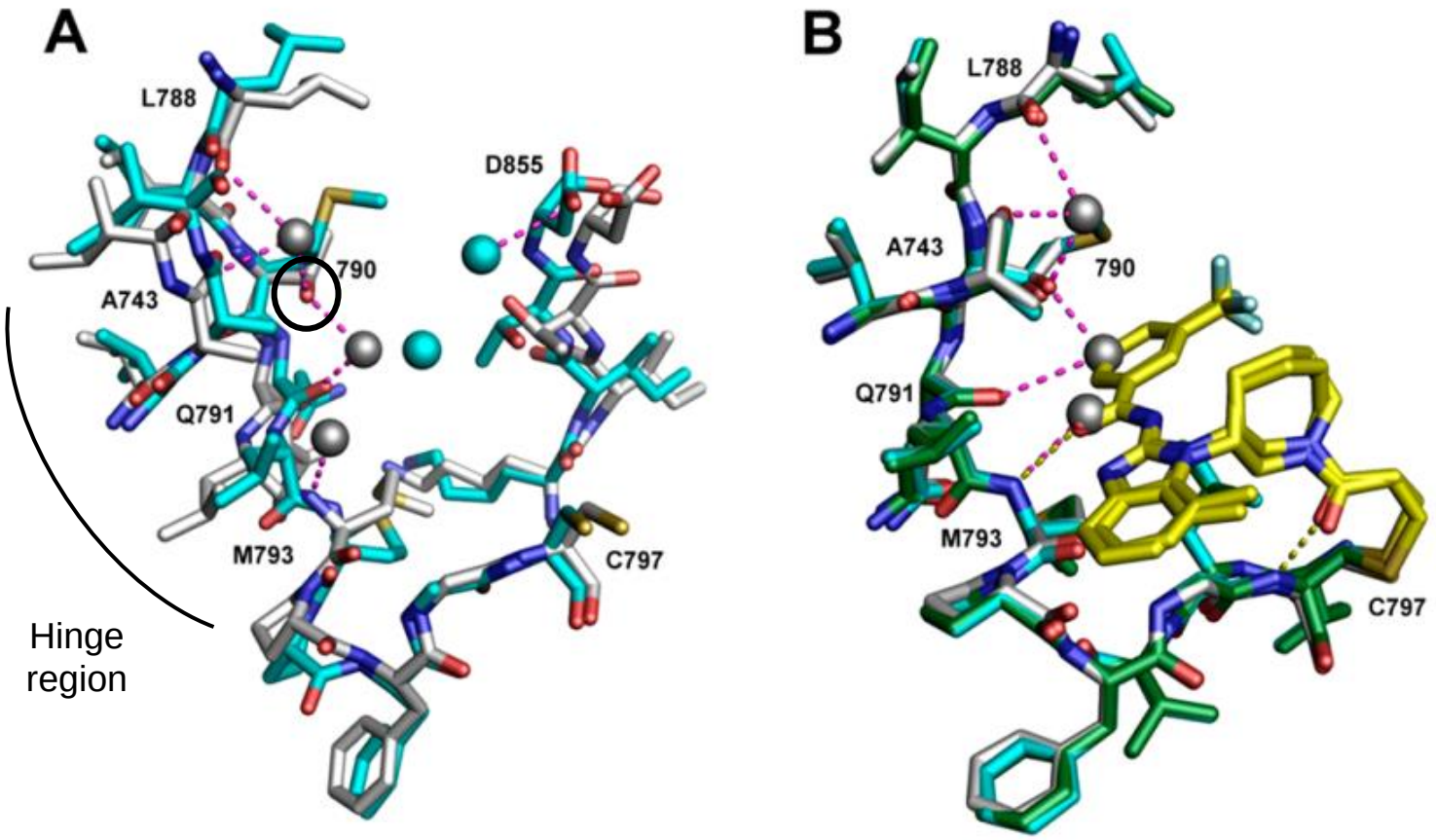

APO **HOLO**

- Holo comparison revealed nearly identical compound conformation
- Apo comparison revealed a network of water molecules in the WT enzyme that is not present in the T790M mutant.
- Binding of the compound to WT EGFR requires the displacement of three strongly coordinated water molecules

Selectivity

- ⊗ Low aqueous solubility (<2 µM)
- ⊗ CYP3A4 and CYP2C9 moderate inhibitor (IC_{50} ~3.5 µM)
- ⊗ Poor oral bioavailability in mice

Design of EGF816 – Lead ADME optimization

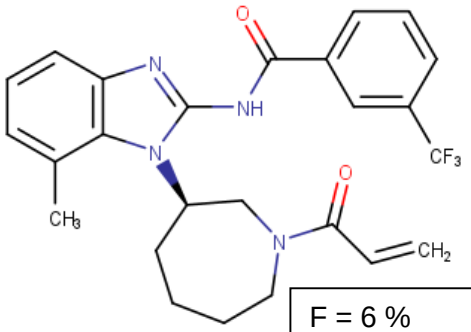

F = 6 %
Sol. = <2 µM
IC_{50} = 1.39 nM

Metabolic Stability

Bioavailability

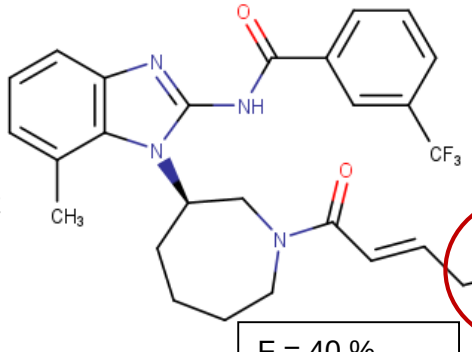

F = 40 %
Sol. = 10.5 µM
IC_{50} = 2.18 nM

Potency

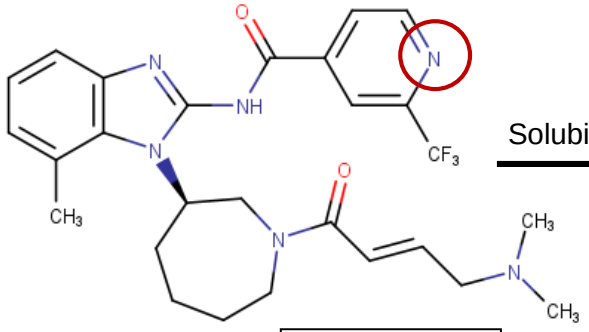

F = 27 %
Sol. = 12.7 µM IC_{50} = 1.51 nM

Solubility

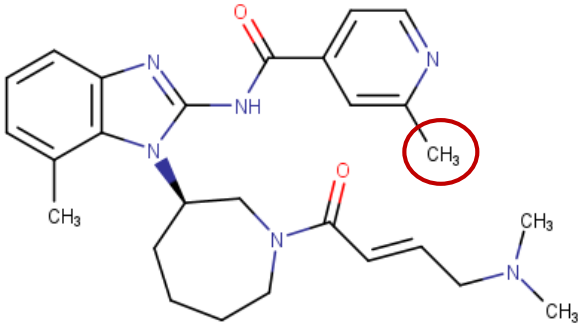

F = 34 %
Sol. = >175 µM
IC_{50} = 2.11 nM

Metabolic Stability

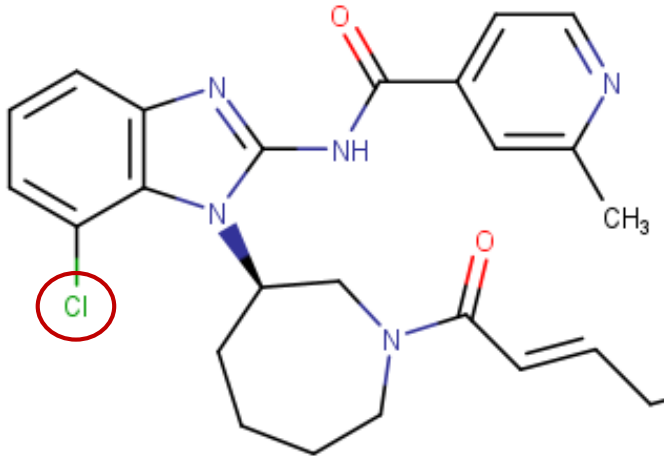

L858R-T790M IC_{50}: 4.18 nM
L858R IC_{50}: 6.11 nM
WT IC_{50}: 160.6 nM

F = 60 %
Sol. = >175 µM

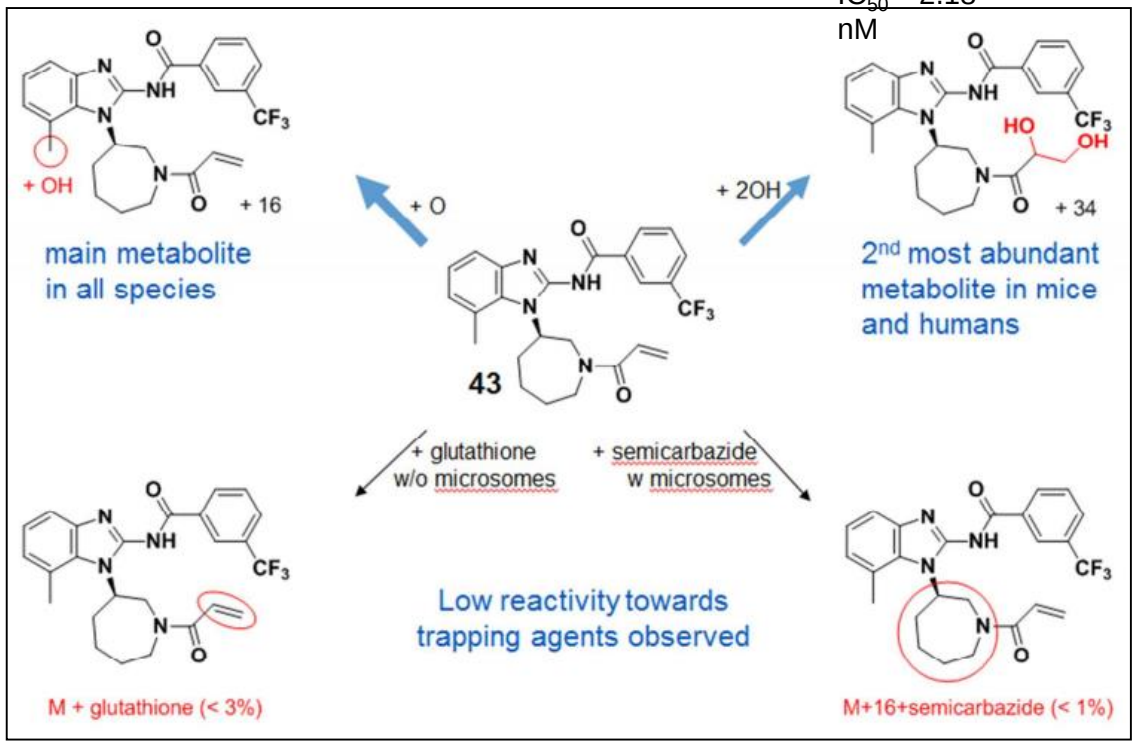

Clinical candidate – EGF816

Nazartinib (Novartis)

Nazartinib – Binding T790M EGFR receptor

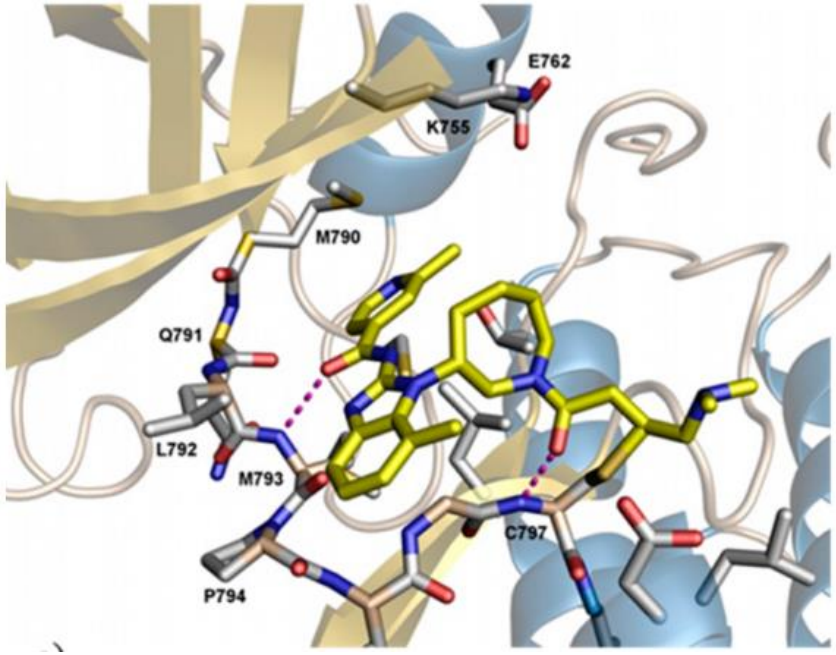

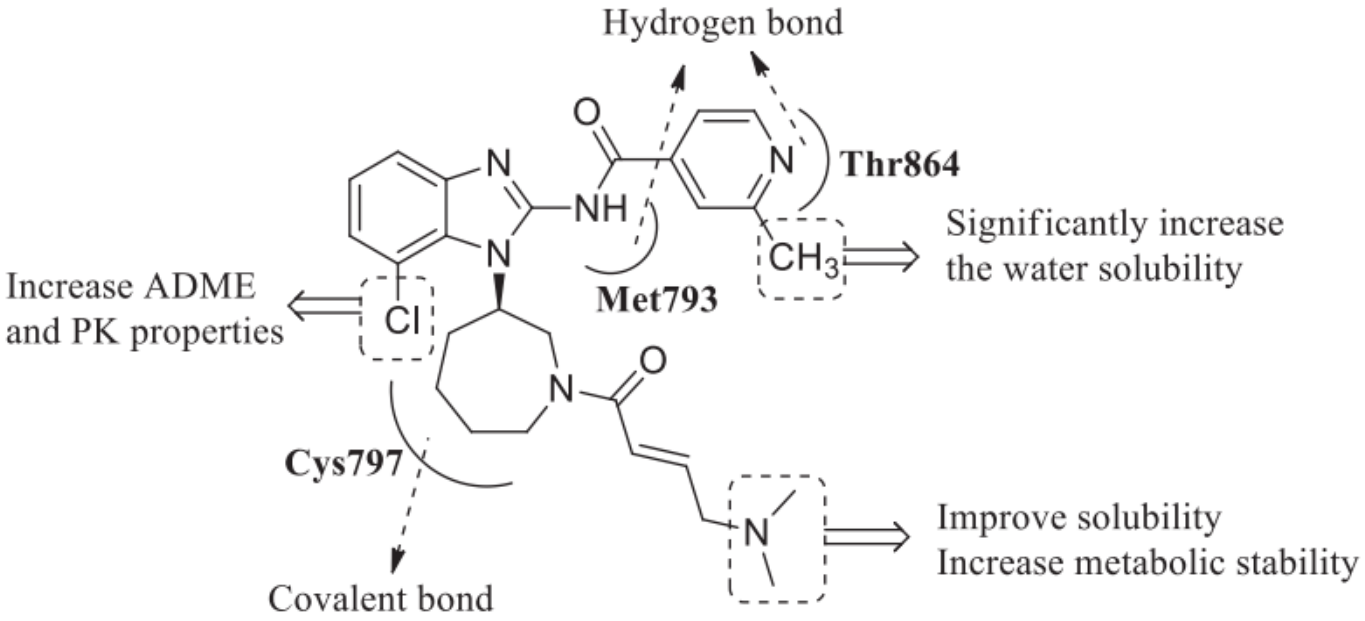

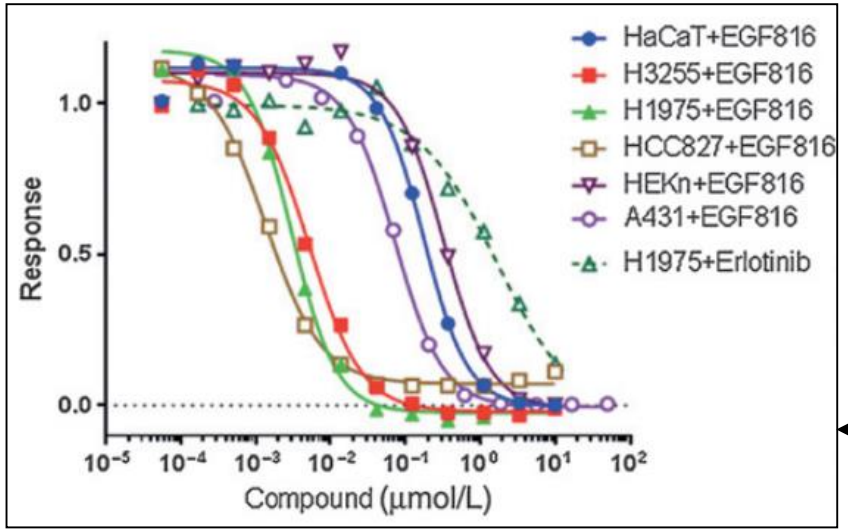

- Cocrystallization of nazartinib with EGFR have not been succesful
- Main interactions with Met793, Thr864 (H bonds) and Cys797 (covalent bond)
- Dose-target modulation relationships in H3255 (L858R), HCC827 (Ex19del), H1975 (L858R/T790M), HaCaT (WT), HEKn (WT), and A431 (WT) cell lines

Nazartinib – *In vivo* preclinical characterization

Short-term *in vivo* efficacy study using a H1975 mouse xenograft model

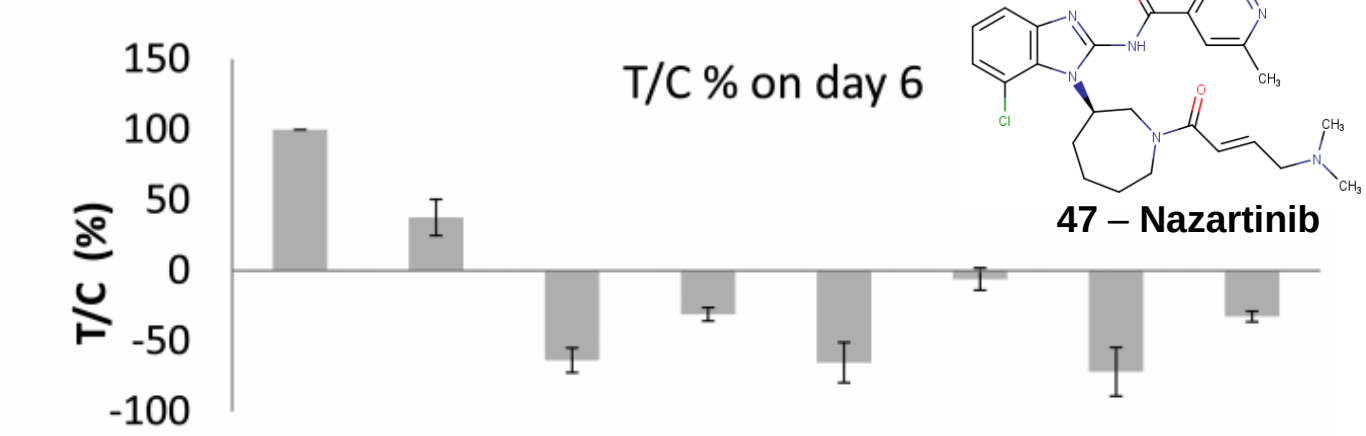

47 – Nazartinib

	vehicle	afatinib	45	45	46	46	47	47
Dose (mg/kg)		25	50	20	50	20	50	25
T/C (%)	100	38	-64	-31	-65	-6	-72	-32
H1975 IC_{50} (nM)		4	1	1	2	2	3	3
Δ (%body weight)	+3.9	-2.4	-3.5	-0.3	-5.0	-1.1	+3.8	+5.3

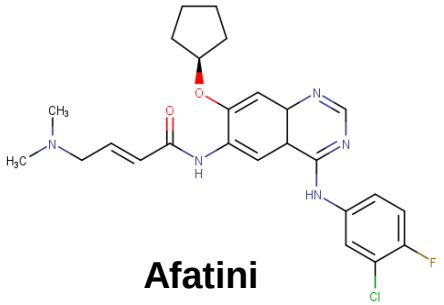

Afatinib

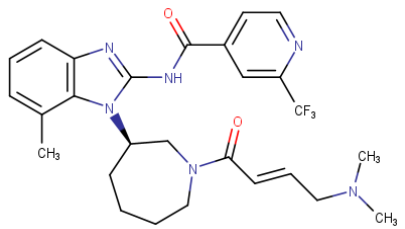

45

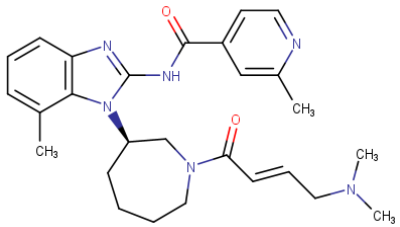

46

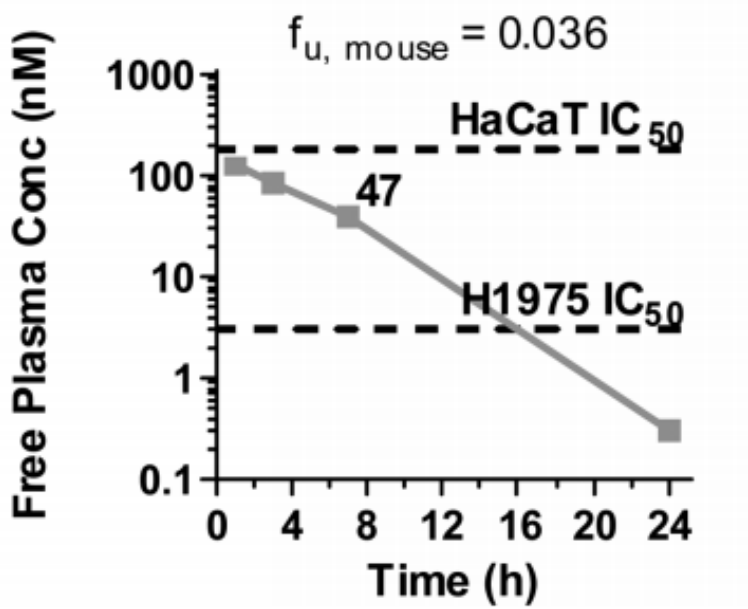

- *In vivo* PK study in mouse, rat and dog
- Nazartinib is predicted to have favorable human PK profile with low to moderate clearance and good oral bioavailability

Nazartinib – *In vivo* preclinical characterization

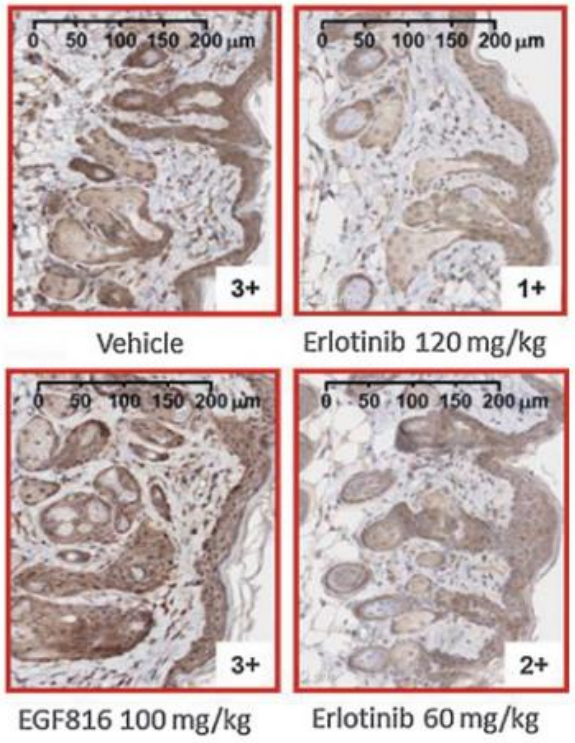

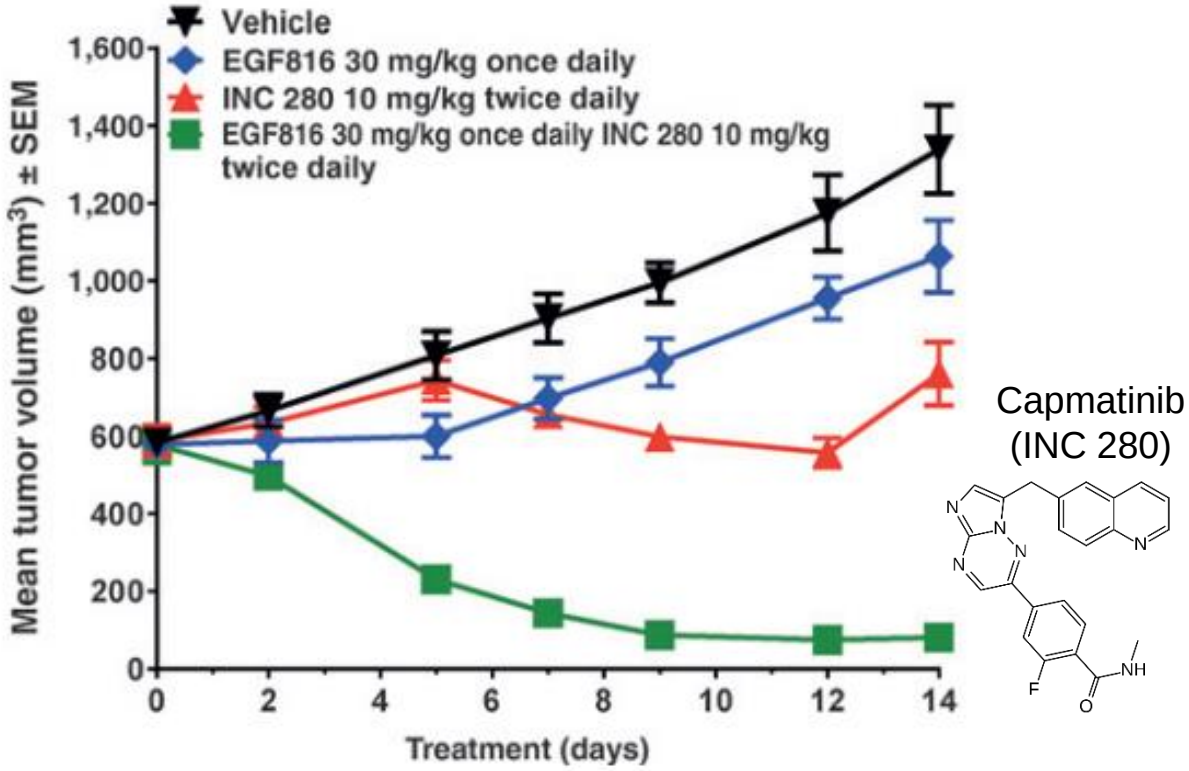

Capmatinib (INC 280)

- IHC staining of WT EGFR in mice
- Even at 100 mg/kg dose EGF816 showed no significant effect on WT EGFR phosphorylation
- Erlotinib showed significant and dose dependent inhibition of WT EGFR

- *In vivo* efficacy in EGF816-resistant HCC827 mouse xenograft model
- Tumour can adapt other escape mechansims to develop drug resistance
- Combination therapies can overcome resistance

Nazartinib – Clinical trials and future perspectives

Phase I	2016 – Safety	NCT02108964

- Manageable safety profile
- Maculopapular rash is an adverse effect characteristic of nazartinib
- No ECG QT prolongation events, against 10% of patients in the osimertinib clinical trial

Phase II	2016 – Effectiveness	NCT02108964

- 69% of patients achieved an overall response and 91% showed disease control
- Median DOR = 25 months, PFS = 18 months and OS = 56 % at 33 months (life expectancy with no treatment is 7 months)
- Clinically meaningful antitumor activity in the brain (CNS recurrence is a frequent complication)

Phase III	2018 – Comparison	NCT03529084

- This is a phase III, open label, randomized controlled multi-center global study designed to evaluate the safety and efficacy of single agent nazartinib (EGF816) compared with investigator's choice (erlotinib or gefitinib) in patients with locally advanced or metastatic NSCLC who are treatment naïve and whose tumors harbor EGFR activating mutations (L858R or ex19del) → estimated study completion date 2024

References

- Abdullah, M.N., Ali, Y. and Abd Hamid, S. (2021) “Insights into the structure and drug design of benzimidazole derivatives targeting the epidermal growth factor receptor (EGFR),” *Chemical Biology & Drug Design*, 100(6), pp. 921–934. Available at: https://doi.org/10.1111/cbdd.13974.
- Das, D., Wang, J. and Hong, J. (2021) “Next-generation kinase inhibitors targeting specific biomarkers in non-small cell lung cancer (NSCLC): A recent overview,” *ChemMedChem*, 16(16), pp. 2459–2479. Available at: https://doi.org/10.1002/cmdc.202100166.
- Hennessey, K. M., Smith, T. R., Xu, J. W., Alas, G. C., Ojo, K. K., Merritt, E. A., & Paredez, A. R. (2016). Identification and validation of small-gatekeeper kinases as drug targets in Giardia Lamblia. *PLOS Neglected Tropical Diseases, 10*(11). doi:10.1371/journal.pntd.0005107
- Hsu, P., Jablons, D. M., Yang, C., & You, L. (2019). Epidermal growth factor receptor (EGFR) pathway, yes-associated protein (YAP) and the regulation of programmed death-ligand 1 (PD-L1) in non-small cell lung cancer (NSCLC). *International Journal of Molecular Sciences, 20*(15), 3821. doi:10.3390/ijms20153821
- Jia, Y. *et al.* (2016) “EGF816 exerts anticancer effects in non–small cell lung cancer by irreversibly and selectively targeting primary and acquired activating mutations in the EGF receptor,” *Cancer Research*, 76(6), pp. 1591–1602. Available at: https://doi.org/10.1158/0008-5472.can-15-2581.
- Lelais, G. *et al.* (2016) “Discovery of (*r*,*e*)-*n*-(7-chloro-1-(1-[4-(dimethylamino)but-2-enoyl]azepan-3-yl)-1*h*-benzo[*d*]imidazol-2-yl)-2-methylisonicotinamide (EGF816), a novel, potent, and WT sparing covalent inhibitor of oncogenic (L858R, ex19del) and resistant (T790M) EGFR mutants for the treatment of EGFR mutant non-small-cell lung cancers,” *Journal of Medicinal Chemistry*, 59(14), pp. 6671–6689. Available at: https://doi.org/10.1021/acs.jmedchem.5b01985.
- Lemmon, M.A., Schlessinger, J. and Ferguson, K.M. (2014) “The EGFR family: Not so prototypical receptor tyrosine kinases,” *Cold Spring Harbor Perspectives in Biology*, 6(4). Available at: https://doi.org/10.1101/cshperspect.a020768.
- Tan, D.S.-W. *et al.* (2020) “Safety and efficacy of Nazartinib (EGF816) in adults with EGFR-mutant non-small-cell lung carcinoma: A multicentre, open-label, phase 1 study,” *The Lancet Respiratory Medicine*, 8(6), pp. 561–572. Available at: https://doi.org/10.1016/s2213-2600(19)30267-x.
- Tan, D.S.W. *et al.* (2022) “Nazartinib for treatment-naive EGFR-mutant non−small cell lung cancer: Results of a phase 2, single-arm, open-label study,” *European Journal of Cancer*, 172, pp. 276–286. Available at: https://doi.org/10.1016/j.ejca.2022.05.023.
- Yun, C.-H. *et al.* (2008) “The T790M mutation in EGFR kinase causes drug resistance by increasing the affinity for ATP,” *Proceedings of the National Academy of Sciences*, 105(6), pp. 2070–2075. Available at: https://doi.org/10.1073/pnas.0709662105.